USING THE CONTINUOUS WAVELET TRANSFORM TO CHARACTERIZE DIFFERENCES BETWEEN IMPACT SIGNALS FROM NON-CLEATED AND CLEATED TURF SHOES

by

Wayne R. Fischer

A thesis

submitted in partial fulfillment

of the requirements for the degree of

Master of Science in Mechanical Engineering

Boise State University

May 2010

BOISE STATE UNIVERSITY GRADUATE COLLEGE

DEFENSE COMMITTEE AND FINAL READING APPROVALS

of the thesis submitted by

Wayne Robert Fischer

Thesis Title: Using the Continuous Wavelet Transform to Characterize Differences between Impact Signals from Non-Cleated and Cleated Turf Shoes

Date of Final Oral Examination: 26 March 2010

The following individuals read and discussed the thesis submitted by student Wayne Robert Fischer, and they also evaluated his presentation and response to questions during the final oral examination. They found that the student passed the final oral examination, and that the thesis was satisfactory for a master's degree and ready for any final modifications that they explicitly required.

Joseph Guarino, Ph.D.	Chair, Supervisory Committee
Michelle Sabick, Ph.D.	Member, Supervisory Committee
Robert Hamilton, Ph.D.	Member, Supervisory Committee

The final reading approval of the thesis was granted by Joseph Guarino, Ph.D., Chair of the Supervisory Committee. The thesis was approved for the Graduate College by John R. Pelton, Ph.D., Dean of the Graduate College.

ACKNOWLEDGMENTS

Sincere appreciation is given to all who have been involved with my engineering studies at Boise State University. In particular, Dr. Joe Guarino has been instrumental in my development and ability to understand the fundamentals of mechanical engineering and the intricacies of vibration and acoustical biomechanics. I would like to also express my gratitude towards Dr. Michelle Sabick, who has always been there to ask me the right questions to lead me to greater discoveries. And a special thanks goes to Dr. Hamilton for reading my thesis draft with a fine comb for detail and overall helpful advice.

I wish to also express my thanks to fellow graduate students, Seth Kuhlman and Wes Orme. Mr. Kuhlman was always very helpful and kind to me when I had important questions to ask about instrumentation at Boise State University's Intermountain Orthopedics Sports Medicine & Biomechanics Research Laboratory and he always had great insight into the biomechanics of running in general. Mr. Orme has been a great colleague in arms as we both forged ahead together into unknown territory, as we both struggled to learn how to apply wavelet analysis in a practical way to the real world. I will always remember those early morning meetings with him and Dr. Guarino to discuss procedures and the meaning of results.

And finally, I cannot forget to thank my lovely wife Betty Miller and all my friends and work colleagues for putting up with my long nights and endless talk about wavelets and how important they are to understand the modern world. Without their love and support and trust I don't think I could have ever completed this thesis.

ABSTRACT

The continuous wavelet transform was used to characterize the time-frequency differences between impact forces from non-cleated and cleated turf shoes among male football athletes who perform cut and run activities. This research is significant because it elucidates how athletes experience different impact force and torque frequency content based on the type of shoe they are wearing.

The complex Morlet mother wavelet was used to analyze all ground reaction force and vertical ground reaction moment signals to create time-frequency power spectrum plots. For each signal, a statistical confidence interval was calculated and displayed along with the cone of influence caused by edge effects. These methods were used to ensure the results to be analyzed were genuine and not a result of edge effects due to the use of the wavelet transform technique or noise from the data acquisition system. To compare and contrast the power spectrum of both cleated and non-cleated turf shoes, a phase angle relationship was computed to find the correlation between the two signals, and then each wavelet transform was sliced at particular frequencies ranging from 11 Hz to 65 Hz to view this correlation at 5 Hz intervals. By calculating the percent difference between the maximum peaks along frequency slices ranging from 11 Hz to 65 Hz, it was possible to identify and characterize differences and similarities between force and moment signals.

In general, but not always, results show that the magnitudes of impact forces are directly related to the magnitudes of low frequency content between 11 Hz and 60 Hz, and the maximum values of the frequency percent differences vary within each GRF

component and the vertical moment plots. For this study, non-cleated turf shoes increase the magnitude and duration of the response from the vertical ground reaction force and this is also particularly true for the medio-lateral ground reaction force and the ground reaction vertical moment of the same style of shoe.

TABLE OF CONTENTS

ABSTRACT iv

LIST OF TABLES vii

LIST OF FIGURES viii

INTRODUCTION 1

Statement of Purpose 1

Hypothesis 7

LITERATURE REVIEW 8

Attenuation of Impact Forces and Mechanisms of Injury 8

Gait Analysis and the Frequency Content of Ground Reaction Forces 11

Time-Frequency Signal Analysis Using the Wavelet Transform 21

METHODS AND PROCEDURES 26

Protocol and Instrumentation 26

Data Preparation 28

Data Analysis 34

RESULTS 39

DISCUSSION 70

CONCLUSION 77

REFERENCES 79

APPENDIX 84

MATLAB Software Programs 84

LIST OF TABLES

Table 1. Overall Practice and Game Injury Rates Per 1000 Athlete-Exposures 4

Table 2. Statistical Comparison of the Mean Peak Vertical Ground Reaction Forces … 39

LIST OF FIGURES

Figure 1. Typical Outsole of Shoes Worn during Athletic Activities 2

Figure 2. Distribution (percentage) of Injuries by Injury Mechanism for Practices and Games Involving 15 Sports 3

Figure 3. Distribution (percentages) of Injuries by Body Part for Games and Practices Involving 15 Sports 3

Figure 4. Turf Toe: Hyperflexion of the Metatarsophalangeal Joint of the Great Toe 5

Figure 5. Midsagittal Section of the Foot 8

Figure 6. The Two Most Important Lateral Ankle Static Stabilizers 10

Figure 7. Mean Transmissibility of Lower Extremity Muscles (Quadriceps, Hamstrings, and Triceps Surae) for Viscous Midsole Condition (solid line) and Elastic Midsole Conditions (dashed line) 18

Figure 8. Simplest Model of the Human Body as a One-Mass-Spring with Damping ... 20

Figure 9. Explanation of Wavelet, Signal, and Transform Plot 22

Figure 10. Complex Morlet Mother Wavelet 23

Figure 11. Mathematical Representation of the Complex Morlet Wavelet 23

Figure 12. Experimental Setup 27

Figure 13. Ground Reaction Force Plates 27

Figure 14. Typical Vertical Component of Ground Reaction Force 28

Figure 15. Z-Axis Averaged Force Signals of Cleat and Turf Shoe for Left and Right Foot (Not the Same Vertical Scale) 30

Figure 16. Y-Axis Averaged Force Signals of Cleat and Turf Shoe for Left and Right Foot (Not the Same Vertical Scale) 31
Figure 17. X-Axis Averaged Force Signals of Cleat and Turf Shoe for Left and Right Foot (Not the Same Vertical Scale) 32
Figure 18. Z-Axis Averaged Moment Signals of Cleat and Turf Shoe for Left and Right Foot (Not the Same Vertical Scale) 33
Figure 19. Wavelet Transform Example Showing Confidence Interval and COI. 35
Figure 20. Example Result of CWT Coherence and Coherence Phase between Two Signals (Right Foot GRF in the Z Direction)..... 37
Figure 21. Example of two CWT plots sliced at 25 Hz. 38
Figure 22. Left Foot Ground Reaction Force in the Z Direction with CWT Analysis 41
Figure 23. Left Foot Z-Force Cross-Sections of Power Spectrum from 11 Hz to 35 Hz . 42
Figure 24. Left Foot Z-Force Cross-Sections of Power Spectrum from 40 Hz to 65 Hz. 43
Figure 25. Right Foot Ground Reaction Force in the Z Direction with CWT Analysis... 44
Figure 26. Right Foot Z-Force Cross-Sections of Power Spectrum from 11 Hz to 35 Hz. 45
Figure 27. Right Foot Z-Force Cross-Sections of Power Spectrum from 40 Hz to 65 Hz. 46
Figure 28. Left Foot Ground Reaction Force in the Y Direction with CWT Analysis..... 47
Figure 29. Left Foot Y-Force Cross-Sections of Power Spectrum from 11 Hz to 35 Hz. 48
Figure 30. Left Foot Y-Force Cross-Sections of Power Spectrum from 40 Hz to 65 Hz. 49
Figure 31. Right Foot Ground Reaction Force in the Y Direction with CWT Analysis .. 50

Figure 32. Right Foot Y-Force Cross-Sections of Power Spectrum
from 11 Hz to 35 Hz. 51
Figure 33. Right Foot Y-Force Cross-Sections of Power Spectrum
from 40 Hz to 65 Hz. 52
Figure 34. Left Foot Ground Reaction Force in the X Direction with CWT Analysis..... 53
Figure 35. Left Foot X-Force Cross-Sections of Power Spectrum from 11 Hz to 35 Hz. 54
Figure 36. Left Foot X-Force Cross-Sections of Power Spectrum from 40 Hz to 65 Hz. 55
Figure 37. Right Foot Ground Reaction Force in the X Direction with CWT Analysis .. 56
Figure 38. Right Foot X-Force Cross-Sections of Power Spectrum
from 11 Hz to 35 Hz. 57
Figure 39. Right Foot X-Force Cross-Sections of Power Spectrum
from 40 Hz to 65 Hz. 58
Figure 40. Left Foot Ground Reaction Moment in the Z Direction with CWT Analysis. 59
Figure 41. Left Foot Z-Moment Cross-Sections of Power Spectrum
from 11 Hz to 35 Hz 60
Figure 42. Left Foot Z-Moment Cross-Sections of Power Spectrum
from 40 Hz to 65 Hz. 61
Figure 43. Right Foot Ground Reaction Moment in the Z Direction with CWT Analysis
..... 62
Figure 44. Right Foot Z-Moment Cross-Sections of Power Spectrum
from 11 Hz to 35 Hz 63
Figure 45. Right Foot Z-Moment Cross-Sections of Power Spectrum
from 40 Hz to 65 Hz 64

Figure 46. Z Force Frequency Percent Difference Between Non-Cleated and Cleated Turf Shoes 66

Figure 47. Y Force Frequency Percent Difference Between Non-Cleated and Cleated Turf Shoes 67

Figure 48. X Force Frequency Percent Difference Between Non-Cleated and Cleated Turf Shoes 68

Figure 49. Z Moment Frequency Percent Difference Between Non-Cleated and Cleated Turf Shoes 69

INTRODUCTION

Statement of Purpose

It is a general assumption that repetitive impact forces from jumping and running are the primary cause of injuries to athletes since they are often on average the magnitude of 2.5-3 times the weight of the individual; however, there has been little research to validate this assumption [1].

One approach to examine this assumption is to view the lower limbs as a highly complicated system of structural elements and connective tissue, and to investigate the possibility that repetitive impact forces are near the frequencies when the mechanical impedance of the leg is minimal, thus leading to injury. The most significant frequencies of impact forces during walking and running are in the range of 10 to 20 Hz and the natural frequency of the soft-tissues in the lower extremity range from 10 and 50 Hz, thus it is possible that these frequencies are near the frequencies when the mechanical impedance of the body is a minimum.

As a result of these mechanical effects, physiological effects will also arise; and most importantly, different types of shoes may influence the lower leg's response to repetitive impacts and increase the magnitude and duration of the mechanical and physiological effects [2]. Hence, the purpose of this study was to develop a procedure to characterize and discern differences between ground reaction force (GRF) and vertical moment signals among male football athletes who perform cut and run activities wearing typical cleated or non-cleated turf shoes as shown in Figure 1.

Figure 1. Typical Outsole of Shoes Worn during Athletic Activities [3].

The initial motivation to describe these differences arose from the summary of a 16 year surveillance (1988-1989 through 2003-2004) of collegiate injuries for 15 sports released in 2007 showing the high incidence of contact and non-contact injuries to the lower extremity of athletes [4]. Figure 2 shows that non-contact injuries account for a large percentage of injuries (17.7% during games and 36.8% during practice). During practice these non-contact injuries are close to the same percentage of injuries during games. Also, as shown in Figure 3, the most common injuries, more than 50%, were in the lower extremities—the most common were ankle ligament sprains [4].

Figure 2. Distribution (percentage) of Injuries by Injury Mechanism for Practices and Games Involving 15 Sports [4].

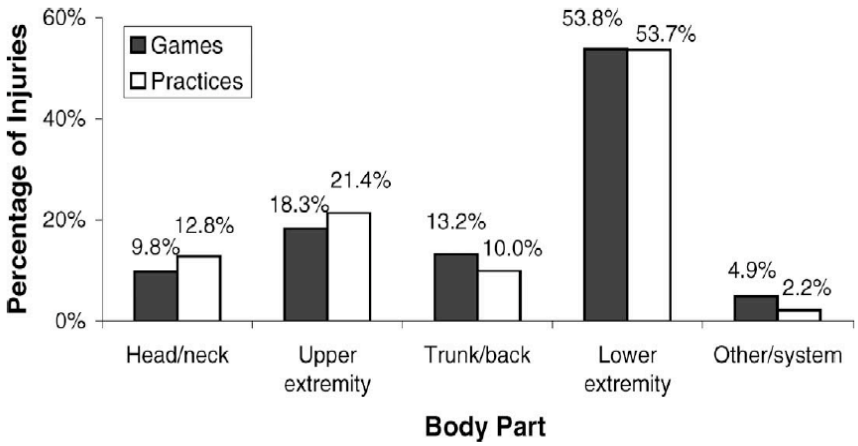

Figure 3. Distribution (percentages) of Injuries by Body Part for Games and Practices Involving 15 Sports [4].

Additionally, the highest rates of injury, during pre-season practice and in-season games, occur in men's football as shown in Table 1 [4]. During practice the injury rate over 16 years was 9.6 injuries per 1000 athlete exposures and during games the injury rate was 35.9 per 1000 athlete exposures [4]. These rates are double the injury rates for men's soccer in both practice and actual games, and the frequency of ankle ligament

sprains is almost three times as high for football players compared to the fifteen other sports [4].

Table 1. Overall Practice and Game Injury Rates Per 1000 Athlete-Exposures

	Practice	Game
Men's spring football	9.6	---
Men's fall football	3.8	---
Men's football	---	35.9
Men's wrestling	5.7	26.4
Men's soccer	4.3	18.8
Women's soccer	5.2	16.4
Men's ice hockey	2.0	16.3
Women's gymnastics	6.1	15.2
Women's ice hockey	2.5	12.6
Men's lacrosse	3.2	12.6
Men's basketball	4.3	9.9
Women's field hockey	3.7	7.9
Women's basketball	4.0	7.7
Women's lacrosse	3.3	7.2
Men's baseball	1.9	5.8
Women's volleyball	4.1	4.6
Women's softball	2.7	4.3

Since the 1970's researchers have been developing varies means to study the causes of athletic injuries. Several factors are involved and can be broken down into three main categories: the physical condition and health of the athlete, the quality of the playing surfaces, and the complicated interactions between the athlete's shoe and the playing surface. These categories are very broad and delving into the details of any one of them and understanding how their qualities interact with one another, and then ultimately finding quantifiable risk factors leading to athletic injuries, is a formidable task.

For instance, contact injuries like the hyperflexion of the first metatarsophalangeal joint (MTP) of the great toe, i.e. turf toe, as shown in Figure 4 have become more common with the use of artificial turf since the 1980's. Annually, an average of five

cases of turf toe incidences are estimated to occur from study findings conducted by the University of Arkansas and Rice University throughout a 14-year period among all sports, but actual turf toe incidences are not clearly defined [5].

Figure 4. Turf Toe: Hyperflexion of the Metatarsophalangeal Joint of the Great Toe [6].

According to Ohlson's and O'Connor's findings, turf toe is the third most common injury after knee and ankle traumas, and accounts for the greatest loss of playing time by athletes [5]. Understanding how the physical conditions of the athlete and the conditions of the playing surface and the type of shoe worn by the athlete and understanding how the shoe interacts with the playing surface can lead to injuries and then using this information to find a way to mitigate these injuries becomes a necessity when you consider the increasingly high cost of surgical procedures to repair the injury, or even more importantly, the high cost of losing an important player from a sport for a season.

Listed in descending order of importance are possible etiological factors leading to a turf toe type of injury identified by Ohlson and O'Connor [5]:

- Footwear: Throughout the past several decades, football shoes have evolved from the traditional 7-cleat shoe containing a metal plate in the sole designed for grass

surfaces to a more flexible, soccer-style shoe designed for grass surfaces and, finally to a shoe designed for artificial turf. These changes have allowed increased speed at the expense of stability. The absence of a stiff sole places the forefoot, and specifically the MTP joints, at much greater risk of sustaining stress-type injuries. Athletes wearing flexible turf shoes are much more prone to injury than are those wearing shoes containing a stiff forefoot.

- Synthetic surfaces: Artificial grass contains a higher coefficient of friction and tends to lose some of its resiliency and shock absorbency over time. The combination of increased surface friction and a hard undersurface is believed to play a major role in the natural history of the injury.
- Ankle range of motion: The risk of turf toe appears to be related to the range of ankle motion in the injured person. A greater degree of ankle dorsiflexion has been correlated with the risk of hyperextension to the first MTP joint.
- Miscellaneous: Player's position, weight, and years of participation, and prior injury.

Although extensive research has been completed and insight into the etiological factors involving athletic injuries has grown immensely, there remains much to be discovered and understood. The first factor listed above concerning footwear has been a general observation of doctors and biomechanical researchers. However, the goal of finding valid quantitative measurements, which can be used to explain and predict leg injuries, remains elusive. Even the effect of adding cushioning to the insoles of shoes is controversial and has been viewed as a so-called "mythic solution" to attenuate impact forces [7, 8].

Hypothesis

The hypothesis of this study is that athletes will experience different impact force and vertical moment frequency content based on the type of shoe they are wearing, and these differences can be characterized using cross sections of time-frequency plots obtained from the use of the continuous wavelet transform.

LITERATURE REVIEW

This literature review is divided into three major sections: 1) Attenuation of impact forces and the prime mechanisms of injury for lateral ankle sprains and turf toe, 2) How the frequency of ground reaction forces have been used to study gait analysis, and 3) How time-frequency signal analysis using the continuous wavelet transform can be used to study gait analysis.

Attenuation of Impact Forces and Mechanisms of Injury

The human body has evolved over several thousands of years and the lower extremity itself has developed the ability to absorb GRF energies at heel strike since the foot, through it unique compartmentalized skin and soft tissues components, acts as a shock-absorbing mechanism as shown in Figure 5 [9] .

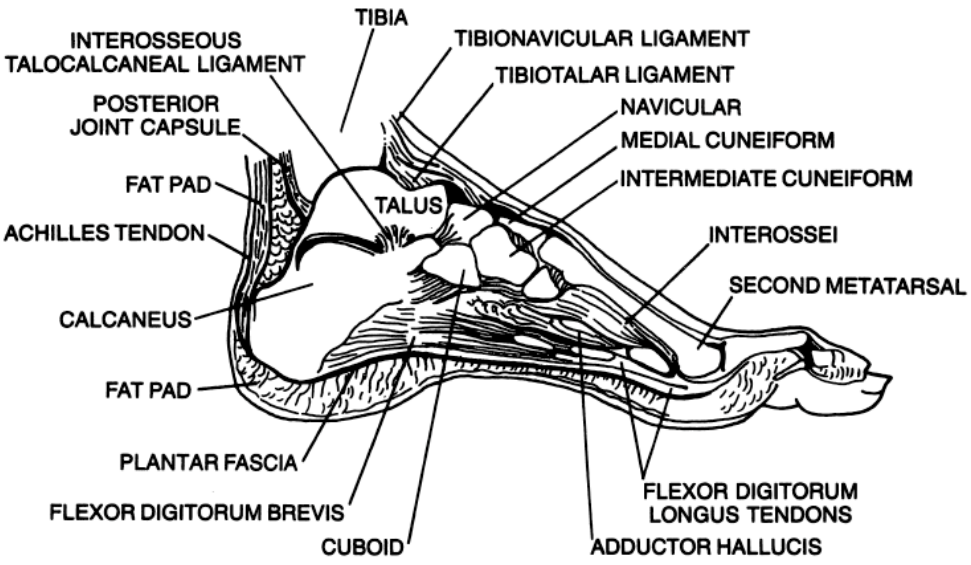

Figure 5. Midsagittal Section of the Foot [9].

The form of the human foot and the ankle, along with the form of the other lower extremity bones and muscles of the human body, has evolved and developed to withstand a high level of physical stress on its structure. Identified potential transient attenuators, according to Gross, include subchondral bones, cartilage, and soft tissue, which support kinematic processes of joints withstanding and dampening sustained impacts and shocks [10]. The foot attachment to the shank, and the large range of ankle motion provide important roles of alleviating shock to the lower limbs and the upper body [10].

Sixty percent of the total gait cycle involves the body going through a stance phase where the heel typically hits the ground first and the foot eventually propels the body forward by pushing off with the front of the forefoot [9]. This repetitive action will eventually cause the body to break down from fatigue and overuse. The most frequent traumas experienced are foot and ankle injuries, regardless of the level of athleticism, and empirical research supports the idea that transient forces dispersed through the skeleton are harmful and contribute to foot and ankle injuries [11, 12].

Even though the body attenuates these forces by tuning the muscles in the lower extremity before ground contact to the correct stiffness, a significant amount of injuries still occur [13, 14]. For instance, 45% of all injuries in basketball, football, soccer, and volleyball are lateral ankle sprains, which typically cause athletes to miss 25% or more of play time in these jumping and cutting type sports, and 40% of these cases end up as chronic disabilities [12].

The mechanism behind these injuries involves the breakdown of one or more muscle or ligament restraints, which provide lateral stability to the ankle. The peroneal muscles provide dynamic stability and play a predominant role in stability if the anterior

talofibular ligament (ATFL), calcaneofibular ligament (CFL), or posterior talofibular ligament (PTFL) become deficient [12]. Shown in Figure 6 are shortened and repaired ATFL and CFL ligaments.

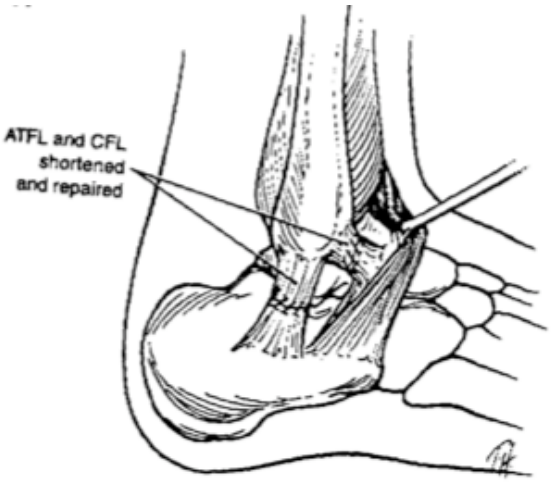

Figure 6. The Two Most Important Lateral Ankle Static Stabilizers [6].

Although the ATFL is the weakest of the three ligaments, it happens to also be the main stabilizer to ankle inversion and lateral ankle sprains. If an injury occurs with great force the ATFL as well as both CFL ligaments may rupture [12].

In conjunction with lateral ankle sprains, during cut and run activities, subtalar joint injuries also commonly occur. The subtalar joint consists of the talus and the calcaneus bones of the foot and ligaments to provide stability. The articulating surfaces of the talus and the calcaneus allow for motion in all three planes, providing an effective mechanical shock absorber and is necessary for normal gait [6]. Often, it is difficult to separate the original site of injury between the ankle and subtalar joint since both cause lateral ankle sprains.

Many reasons for injury and a resulting subtalar sprains may be provided, but according to Mullen, a clinical sports physician, the most common cause is believed to be

dorsiflexion and supination of the foot during extreme positions of the ankle, causing the various ligaments to tear [6]. This study notes that indoor cutting and jumping athletes are the most at risk for subtalar injury.

In addition to lateral ankle sprains and subtalar joint injuries, hyperextension of the first metatarsophalangeal joint of the great toe, known as turf toe, is an ever-increasing athlete injury, resulting in a tear of the metatarsal joint capsule at its insertion onto the metatarsal neck and a compression injury to the dorsal articular surface of the metatarsal head [6]. According to this study, there are different mechanisms for turf toe injuries. For instance, during a football game when an athlete's heel is elevated and another player lands on the back of the foot, a hyperextension injury may occur to the forefoot.

The same study notes that artificial turf and shoe wear are additional factors correlated with a higher incidence of turf toe. Although artificial turf loses its ability to absorb impact forces with age, installation of new turf does not change the incidence of turf toe injuries. However, artificial turf has been identified as a contributing factor to these injuries [6]. Another risk factor for turf toe incidences is the stiffness of the shoe worn by the athlete. Shoes with a flexible forefront allow increased motion of the metatarsophalangeal joint, which provides less resistance to hyperextension forces [6].

Gait Analysis and the Frequency Content of Ground Reaction Forces

Overall, several factors must be included and incorporated into our understanding of how the body attenuates impact forces from running and jumping. Factors such as how different types of surfaces influence the attenuation of impact forces, how different types of shoes interact with these surfaces, and most importantly biomechanical and

biodynamic factors of the human body must be fully explored to comprehend how the body attenuates impact forces.

A fundamental method used to provide an objective and clinically useful technique to study these various factors has been the use of a force plate to measure forces between a foot and the ground. The first force plate was introduced to provide these measurements by Amar in 1916 and continuous development since this time has made these devices widely available [15]. However, very little use of the device was put in place until the early 1980's. One of the first clinical uses of the force plate was completed in 1980 by Jarrett et al when they developed a technique using the components of the ground reaction forces to routinely and objectively assess gait [15]. In their clinical method they used various parameters from the vertical and the anterior-posterior GRF components. For the vertical force they measured parameters such as: 1) peak force after heel strike, 2) peak force before toe off, 3) force minima, 4) loading time to peak force after heel strike, 5) time from peak force before toe off to toe off, 6) duration of stance phase, and 7) the time the force is above body weight [15]. For the anterior-posterior component the parameters used were: 1) minima and maxima force points within the signal, 2) time from heel strike to the first minima, and 3) the time from the maxima to toe off [15].

A year later in 1981 Simon et al was one of the first groups of researchers to use force plates with the intent to re-examine the frequency range of the vertical GRF during normal gait (with and without shoes) since the last research had been completed in the mid 1950's and 60's [16]. Their intent was to find out if the impact forces consisted of only low frequencies or whether or not higher frequencies above 20 Hz might be present during the shock at heel strike [16]. Using Fourier analysis of the vertical GRF they

found that majority of the frequency content of signals exist below 10 Hz, but some higher frequencies also exist up to 75 Hz without shoes and up to 50 Hz with shoes [16].

Simon et al note that the velocity and angle of heel strikes are contributing factors to the higher frequency findings, but they also conclude that soft tissues in the foot and the footwear worn affects the levels of severity experienced from high frequency impact loads [16].

A few years later in 1987, Munro et al completed one of the next major developments using GRF data that was important to understanding the gait of athletes. They collected data on adult males running at speeds from 3.00 to 5.00 meters per second wearing typical jogging shoes to establish a normative standard of the typical gait of runners using common parameters such as impact peak, loading rate, the average vertical GRF, and the change in vertical velocity [17]. Also to visually demonstrate the magnitudes of the forces through time at various speeds, Munro et al. created 3-dimensional plots [17].

Although this study was able to establish vertical and anterior-posterior GRF norms, medial-lateral GRF descriptor variables were not identified and GRF frequencies were not analyzed [17].

Similar time-domain GRF research continued throughout the 1980's and 1990's to analyze gait. For instance in 1998, Begg et al. used GRFs in the time domain to study kinetic and kinematic adaptations made to overcome obstacles and understanding gait control processes occurring in normal walking humans [18]. Frequency content of the GRF was not used in this study, but data were collected on both feet. Force-time data revealed the "trail foot [compared to the lead foot] generated greater vertical and anterior-

posterior force during the push-off/propulsive phase across all obstacle conditions" and in addition, the trailing foot had "lower vertical peak force during mid-stance and produced greater vertical and anterior-posterior impulses" [18]. Although these findings are for normal walking individuals, the results are still important to know when interpreting the cut and run GRF signals from athletes.

By the late 1980's, low mass accelerometers along with force-plate and high-speed cinematography were non-invasive methods for approximating impact-generated transients. With these devices it was possible to investigate in more detail and varied ways the kinematic data that might reveal the shock attenuation role of the ankle during a landing from a vertical jump [10]. In their 1988 study, Gross and Nelson examined the role of the ankle in the shock attenuation process. By using accelerometers during barefooted vertical jumps onto three different types of ground cushioning, the skin covering the calcaneus and distal anterior-medial portion of the tibia were examined [10].

The most important result from these measurements was that the range of cushioning for the ground did not significantly alter the shock attenuation effect; rather, they found that kinematic patterns, along with bone, cartilage and tissue factors governed the damping of impact.

Another interesting result from their study was that there were two distinct landing styles. In one case the heel contacted first during the landing, and in the other case the subject produced a more controlled lowering of the heel. The non-heel contact landers experience little or no contact for the cushioning phase and skeletal transients, which may prevent joint degeneration and long-term injury [10].

In 1989, Kandarp Acharya wrote one of the first articles describing a method to measure the force magnitude and the spectral frequency content of the heel strike during a typical gait cycle. Acharya and his research group were interested in understanding how exposure to hypogravity produces a degenerative response in bone, and consequently they were in search of finding the optimum magnitude and frequency of stress to support normal bone remodeling under normal gravity conditions [19]. Using basic Fourier analysis they found that all frequency content of interest lies below the 40 Hz mark and the Fast Fourier Transform magnitude is consistently higher than 40 Hz, approximately 0.2% of the time [19].

In the late 1990's, Giakas and Baltzopoulos wrote one of the first papers using time and frequency domain analysis of GRF signals during normal walking. This study showed that the appropriate use of GRF comparison procedures would be to examine GRF curve frequency patterns, rather than isolated time domain parameters [20]. They used Fourier analysis on GRF signals because they felt that when a clinician compares normal and pathological gait signals, it is more important to examine the development and oscillation of forces throughout the gait cycle rather than isolated time domains [20]. Giakas and Baltzopoulos also concluded that the development of established and normal waveforms can enable the detection of pathological conditions [20].

Consequently their overall objective was to investigate and verify past studies of the symmetry between left and right lower extremities during the support phase of normal human gait by analyzing the time and frequency content of GRF signals of normal walking subjects [20]. Since variability between subjects is an important factor involved in GRF comparisons they were also concerned with studying variability between signals

using time and frequency parameters since any signal analysis method used would involve this phenomena [20].

In their study they used a sampling frequency of 200 Hz because other researchers had found a power spectrum of GRF data revealed an average of 98% of their content to be below 100 Hz, and others found that a high frequency spike early in heel strike existed and varied from 10 to 75 Hz [20].

Giakas and Baltzopoulos arrived at five major conclusions from their study [20]:

1) The frequency content and the variability of left and right sides within the same component are similar, and this was confirmed using both time and frequency analysis.
2) The medial-lateral component contains more oscillations compared with the other two components, which is evident in force-time patterns, but clearly numerically expressed with Fourier analysis.
3) It was found that the development of forces throughout the gait cycle remains consistent and this was true for all three GRF components.
4) The determination of a single subject's force-time pattern as representative is inappropriate due to intra-subject variability and selected time domain parameters in the medial-lateral direction, especially during pronation, contains substantial variability and should not be used as a criterion of normal gait.
5) Their hypothesis that normal gait is a symmetric movement was confirmed only with the use of Fourier analysis, while substantial asymmetries characterized time domain variables in the medial-lateral component.

From results like these, researchers were then able to clinically use the frequency domain of GRF signals for gait description and characterization. For instance, in 2002, Stergiou et al characterized differences in the gait of young and elderly females [21].

In addition to these developments a significant paper was written by Nigg in 2001, when he developed and revealed a new paradigm called Muscle Tuning that involves impact forces and movement control and tries to explain contradictions in heel to toe running observations [13]. The new perspective claimed that impact forces are not the primary factors in the development of chronic and/or acute running-related injuries, but rather, impact forces during running "are input signals that produce muscle tuning shortly before the next contact with the ground to minimize soft tissue vibration and/or reduce joint and tendon loading" and it is through this repetitive action of muscle tuning that affects fatigue and performance [13]. Ultimately, over time, the body is not capable of optimizing its tuning ability, and this is what leads to lower limb injuries.

To support this paradigm, Wakeling, Nigg, and Rozitis showed in 2002 through mechanically pulsed and continuous vibrations that the properties of the soft tissues in the lower extremities are changed in response to the input frequency content given to the body [14]. By subjecting individuals to a vibrating platform driven by a hydraulic actuator, across the frequency range of 10 to 65 Hz, and measuring soft tissue responses using accelerometers and muscle activity using surface electromyography devices on the main muscles of the lower extremities, they were able to show that increased muscle activity and increased damping of vibration power occurred when the input frequency was close to the resonant frequency of each soft tissue; but, the soft tissue resonant frequency did not change in a related way with the frequency of the input [14]. From

these results it was concluded that resonance is minimized during initial impact through the mechanism of soft tissue damping [14].

Overall, there have been many developments over the past several decades that help us understand how the body attempts to attenuate repetitive impact forces. We have learned that typical impact forces have a frequency range of 10 to 20 Hz and these frequencies produce soft tissue vibrations in the body [22]. By 2006, methods to measure impact forces and spectral frequency had advanced, and in Boyer and Nigg's study on the implications of an untuned landing they were able to conclude that typical impact frequencies can vary substantially between subjects (14.8 to 25.4 Hz) and the magnitude of change among subjects varied by 0 to 5 Hz [23].

In addition to knowing the general GRF magnitudes through time and frequency, it has been found by Wakeling et al that the resonant frequencies of the soft-tissues in the lower extremity range between 10 and 50 Hz [24]. These frequency ranges have recently been empirically supported by Boyer and Nigg's research showing the mean transmissibility of three major muscles groups of the lower extremity, as shown in Figure 7 to be around 11 and 35 Hz for the quadriceps, hamstrings, and the triceps surae [25].

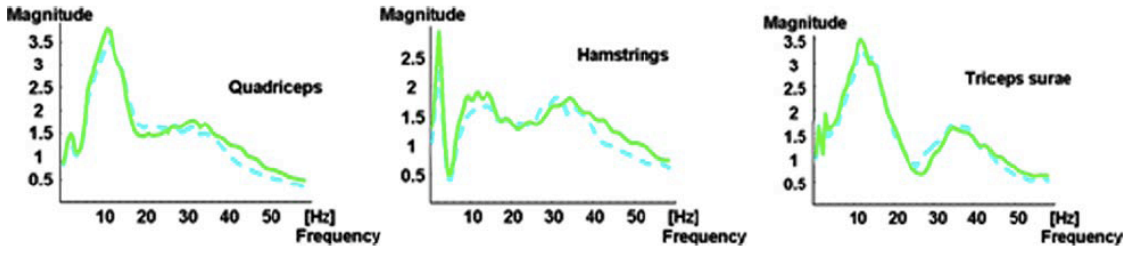

Figure 7. Mean Transmissibility of Lower Extremity Muscles (Quadriceps, Hamstrings, and Triceps Surae) for Viscous Midsole Condition (solid line) and Elastic Midsole Conditions (dashed line) [25]

Consequently, in contrast to viewing the ground impact forces to be in resonance with the bones of the body, which typically have resonant frequencies above 100 Hz, it is possible that these lower frequencies are near the resonant frequencies of the soft tissues of the lower extremities or near the frequencies when the mechanical impedance of the body as a whole is a minimum [14, 26-28]. It is also known that the fatigue strength of bone at frequencies below 50 Hz has not been researched and that stress frequencies above 30 Hz results in increased fatigue life [29].

At this point we should keep in mind Griffin's comment in his introduction to the study of whole-body biodynamics in the *Handbook of Human Vibration* [30]:

> While the investigation of resonances is interesting, the use of 'magic numbers' to summarize knowledge of the dynamic response of the body is of little help: the dynamic response of the body must be considered as a continuous function throughout the range of frequencies of interest.

Attempting to view the repetitive impact GRF signals as the primary factor leading to potential mechanical failure is like focusing too much on the details of the trees in the forest rather than seeing the forest for what it is, and this can lead to the assumption that all damaging effects of vibration can be predicted from measurements of the vibration transmitted to or through the body.

To assume that single point impedance or transmissibility measurements will predict all frequency responses is to assume that these responses are mainly dependent on a single unit of vibration, yet injuries like high ankle sprains or turf toe injury incidents are not easily predicted because many factors are involved [30]. Consequently, it is important to realize that the effects of repetitive impact forces viewed as GRF signals with a certain

frequency range are dispersed throughout the body and that single point transmissibility measurements are over simplifications of complex frequency responses [30].

So it must be understood and underscored that modeling the lower limb as a single-mass with a dash pot and spring, as shown in Figure 8, is an extremely over simplified biodynamic perspective of the lower limb and that the lower limb has a very complex dynamic response and must be viewed as a highly complicated system of interconnected masses, elasticities and viscous dampers that probably includes many resonances [30]. It is even very unlikely that single axis information can be easily transferred to a multi-axis situation as Holmlund and Lundström demonstrated in their investigation of the mechanical impedance of the sitting human body exposed to a range of low frequency vibrations [31].

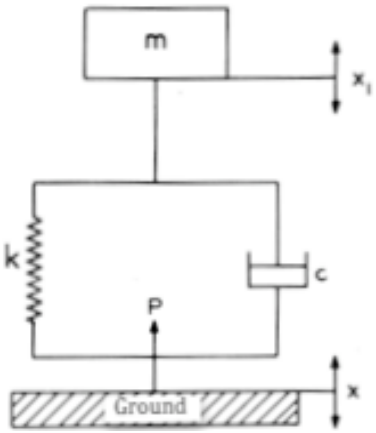

Figure 8. Simplest Model of the Human Body as a One-Mass-Spring with Damping [2]

Given this awareness of how complex and complicated it is to fully comprehend the effect of low frequency repetitive impacts on the human body and the lower limb, it is also important to realize that using plots of the GRF magnitudes through time and analyzing their frequency domains has been a useful and practical way to describe the biomechanical and biodynamic parameters necessary to analyze how the body attenuates impact forces.

The next step toward adding to this knowledge is to combine the ability of viewing GRF signals as either time or frequency domains into one method where magnitude, time, and frequency of GRF signals can be plotted and analyzed.

Time-Frequency Signal Analysis Using the Wavelet Transform

Classical spectrum analysis mainly consists of using Fourier Transforms and Short-Time Fourier Transforms. As is commonly known, these methods break a signal down into constituent sinusoids of different frequencies and corresponding coefficients reflect the magnitude of those frequencies. Although Fourier analysis is a powerful analytical tool to find the dominant frequency of a signal, its weakness is that it does not provide localized information concerning when a particular dominant frequency occurs. Short-Time Fourier analysis (the Gabor transformation) attempts to overcome this weakness by windowing the area of interest; however resolution problems are then encountered much like zooming in on a low resolution picture [32].

A wavelet transform is a relatively new mathematical tool that can be used to process signals and provide salient information about both the time and frequency content of a transient signal because it uses a waveform pattern of limited duration that has an average value of zero in contrast to a sine wave, which has a unlimited duration [32, 33].

Wavelet analysis consists of taking a waveform, such as the complex Morlet wavelet used in this study, and moving it through the extent of the signal. Illustrated in Figure 9 below, as the waveform is stretched out and scaled, coefficients are produced as a function of both scale and position, representing how well the waveform matches the signal [32].

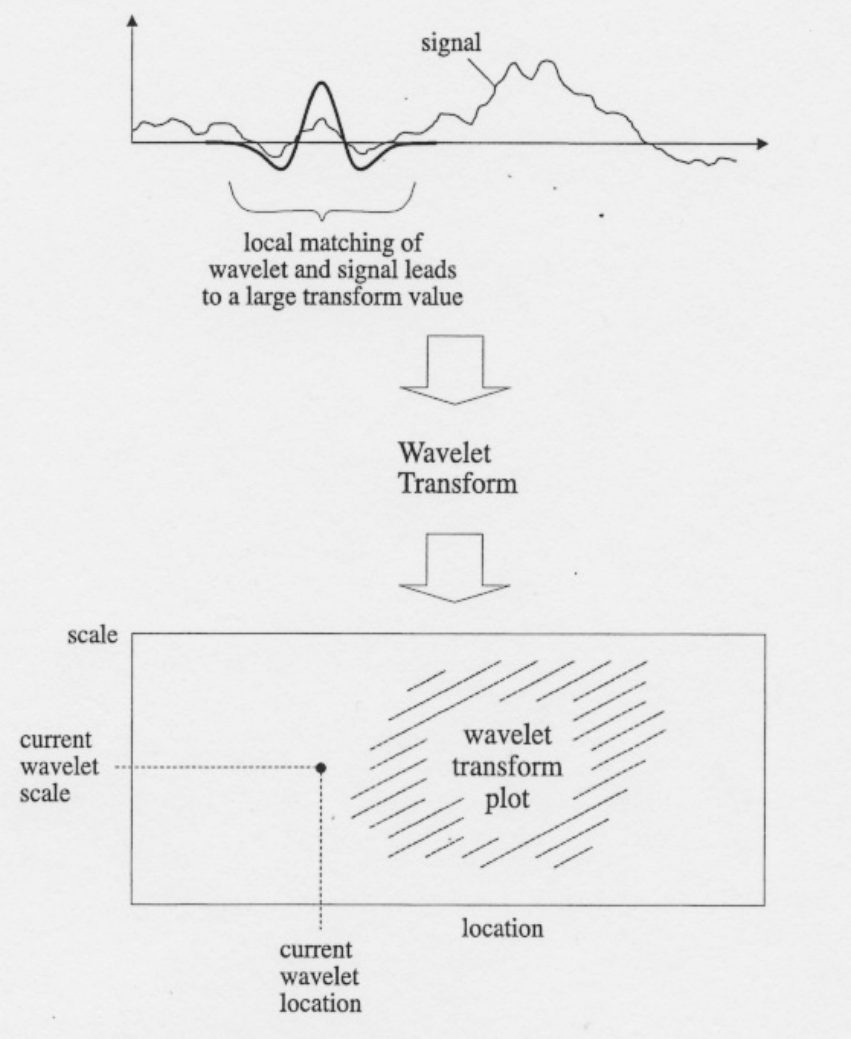

Figure 9. Explanation of Wavelet, Signal, and Transform Plot [33]

Two main classifications of a wavelet transform exist: the discrete wavelet transform (DWT) and the continuous wavelet transform (CWT). DWT's use a specific subset of all scale and translation values; whereas, CWT's operate over every possible scale and translation values. DWT's are commonly used in pattern recognition and image compression processes since the discrete subsets can be convoluted and the results can reproduce a compressed copy of the original signal by using only pertinent information. Signal analysis engineers use CWT's since the desired outcome is not to reproduce the

original signal, but rather to analyze it at all possible scale and translation values.

Although there can be an infinite amount of wavelet waveform patterns, the complex Morlet wavelet, as shown in Figure 10, was used since it provides a precise pseudo-frequency because the wavelet scale value "a" is approximately equal to the Fourier period, and it could also provide phase information about the signal [34].

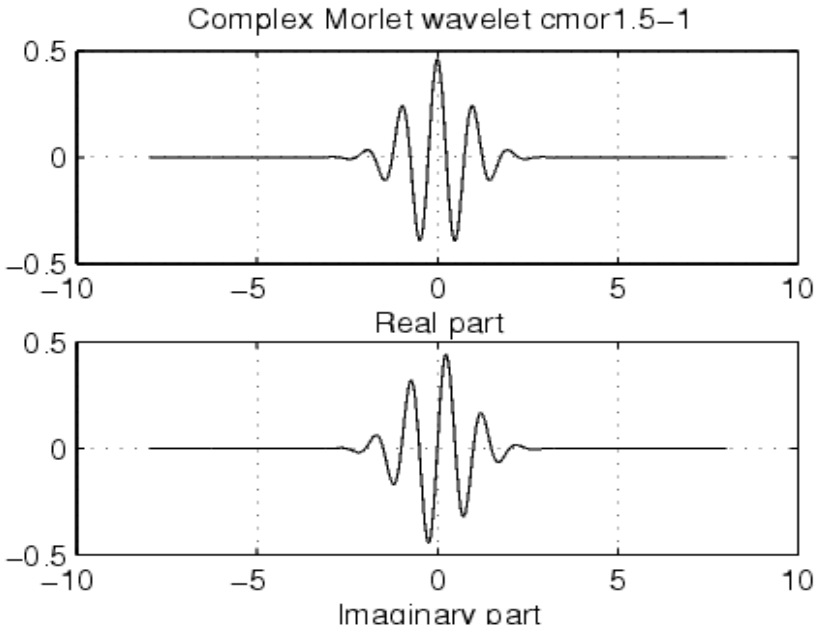

Figure 10. Complex Morlet Mother Wavelet [35]

The mathematical representation of the complex Morlet wavelet is shown in Figure 11 below.

$$\psi(t) = \frac{1}{\pi^{1/4}} e^{i2\pi f_0 t} e^{-t^2/2}$$

normalization factor — complex sinusoid — Gaussian bell curve

Figure 11. Mathematical Representation of the Complex Morlet Wavelet

As a consequence of the Heisenberg uncertainty principle, a wavelet transform has good time but poor frequency resolution at high frequencies, and good frequency but poor time resolution at low frequencies. As long as the necessary conditions are taken into consideration, then the wavelet transform becomes a powerful tool for time-frequency analysis of signals.

The first instance where a wavelet transform was used to represent GRF data was in 1996 by Sloboda and Zatsiorsky [36]. In their article, given at the proceedings of the ASME Dynamics Systems and Control Division conference, they proposed the use of the discrete wavelet transform as a way to discern how various frequencies are involved in the immediate impact forces; most importantly, they were able to characterize the differences in energy of two vertical GRF signals using these frequency ranges [36].

At the end of their article they noted how the use of wavelets may become a useful tool in biomechanical research because the majority of signals gathered in biomechanical research are aperiodic and non-stationary, which wavelets were specifically designed to study in contrast to Fourier analysis which is well suited for representing periodic stationary processes [36].

The next successful use of the wavelet transform to analyze ground reaction forces was by Verdini and his group in 2000 [37]. The objective of their research was to identify details of clinical relevance in ground reaction forces through the use of a wavelet transform. They carried out a retrospective study of gait analysis using a wavelet transform by tiling the amplitude of the coefficients to represent the percentage of energy contained within the signal at particular frequencies and moments [37]. They analyzed all ground reaction forces using the wavelet transform and the result was the ability to detect

the sharp transient frequency content during the first part of the stance phase [37]. This result allowed the researchers to view the time-frequency ability of the wavelet transform as a potential tool to use for clinical assessment or treatment analysis [37].

By 2006, Verdini and his group had developed and automated their analysis technique using the wavelet transform and used it to identify and characterize heel strike transients of normal walking subjects [38]. For their study they gathered lower limb kinematics, and kinetic and surface electromyography data of subjects walking barefoot over a force plate. The result of the study was the ability to reliably identify a heel strike transient in the vertical and anterior-posterior components of the GRF for 76% of the subjects. They plan to use the results from this normal standard to investigate heel strike transient patterns in subjects with pathological gaits.

In summary, this literature review has discussed how the body attenuates impact forces and possible mechanisms to lower limb injuries, and how the use of ground reaction forces along with their frequency content has been used to study how the body attenuates impact forces and gait analysis. Along with many other parameters, researchers have used GRF magnitudes and have begun to analyze their frequency contents, using Fourier analysis, as a way to describe how the body attenuates impact forces. What has not been fully developed yet is the use of time-frequency signal analysis using the CWT to study gait analysis, nor has there been much research done to explain how the various GRF frequency differences might influence injury mechanisms.

METHODS AND PROCEDURES

Protocol and Instrumentation

Eight active Division I collegiate male football athletes participated in this study. Their weight was (mean +/- SD) 807.5 +/- 103.9 N and their ages ranged from 18 years old to 25 years old. All eight subjects were running backs or receivers. At the time of the experimentation, they were free of pain and injuries to their lower extremities and the Boise State University Human Subjects Research and Institution Review Board approved the experimental protocol.

Athletes performed two-footed jumps, upward and forward over a level bar set at 15 inches off the ground. The athletes landed with their feet on the centers of two ground-level force platforms situated under artificial turf, then sprinted unanticipated off the force plates to a target located either straight ahead, or approximately 30 degrees to the right or left. Subjects were not aware of the direction of their sprint until they passed over the bar, at which time they were signaled the direction of their run by an electronic beacon. Three trials per subject in each direction with 30-second intervals per trial were obtained. In this study only the straight ahead (center) cut and run data sets were analyzed to simplify analysis.

Figure 12. Experimental Setup

The main features of the measuring system are shown in Figure 13. The multi-component ground reaction forces plates and data acquisition software was purchased from Kistler Instruments. Force plates are model number 9281C with vertical and transverse resonant frequencies of 1000 Hz. Each plate is 400 mm wide and 600 mm long, and they were separated by 3 mm. The force plate reactions (including force and moments along the Z, Y, and X-axes) for both feet were recorded using BioWare at a sample rate of 1250 Hz [39].

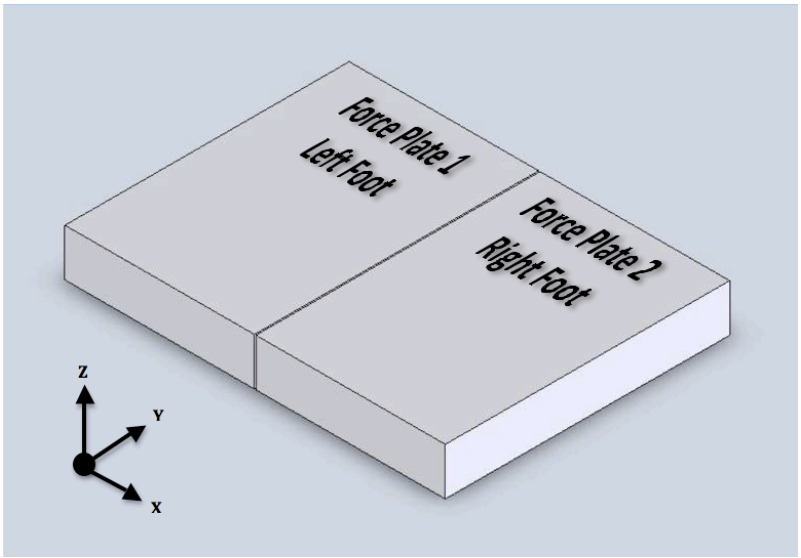

Figure 13. Ground Reaction Force Plates

Data Preparation

A typical pattern of the vertical ground reaction force is shown in Figure 14. Only the impact portion of the signal was used in this study to simplify analysis and results. The impact point for each trial run was located by viewing the first dramatic point of change in the vertical force component. The signal was then pre-value padded out from this point by 125 sample points and then post-value padded out from the first minimum of the vertical force to achieve a standard sample space of 500 samples, equivalent to 400 ms. Although only 50 ms of genuine activity takes place within this sample space, this size was necessary to accommodate for border effects involved in the data analysis process described later. This initial impact point was used to align the additional force and moment data along the Z, Y, and X-axes to a common reference point.

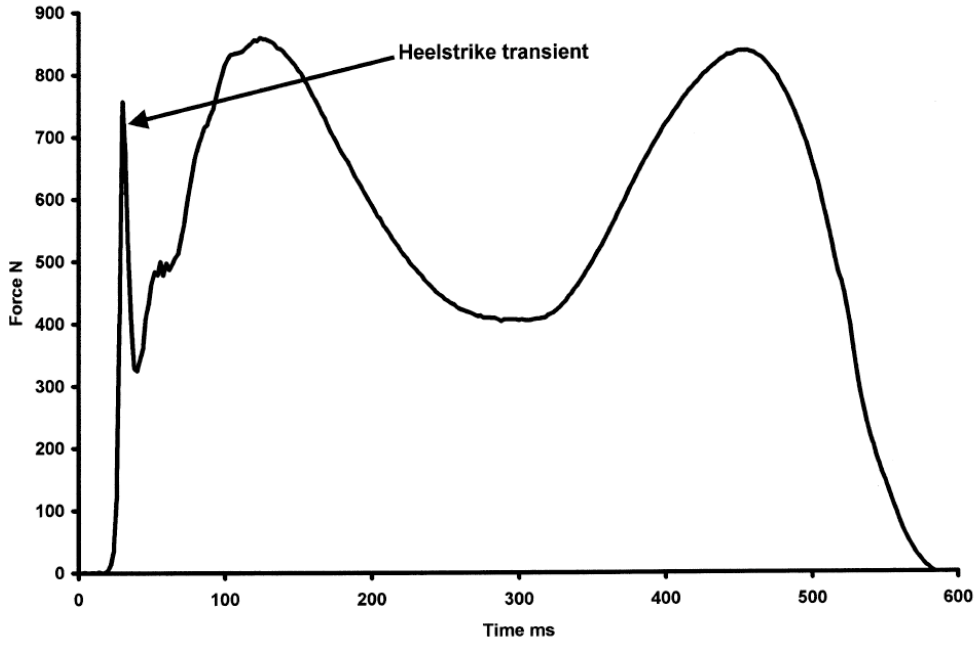

Figure 14. Typical Vertical Component of Ground Reaction Force [11].

The force-time data was then normalized by dividing each force component by body

weight to make it possible to compare force magnitudes across subjects independent of body weight. Only the moment data along the Z-axis was used to analyze due to the inability to control the landing position of the subjects.

And finally the three trials from each subject were averaged, and each of these signals was then averaged as a total since there is not a standard to which individual trials can be compared and judged. This procedure may cause nuances in the data to be washed out; however, since this is a preliminary study, this averaging procedure allows for a global perspective of the data. The overall result was a single force signal for each GRF axes, and a single moment signal along the Z-axis for both the left and right foot of all 8 subjects. Plots of the averaged force and moment signals are shown in the following pages.

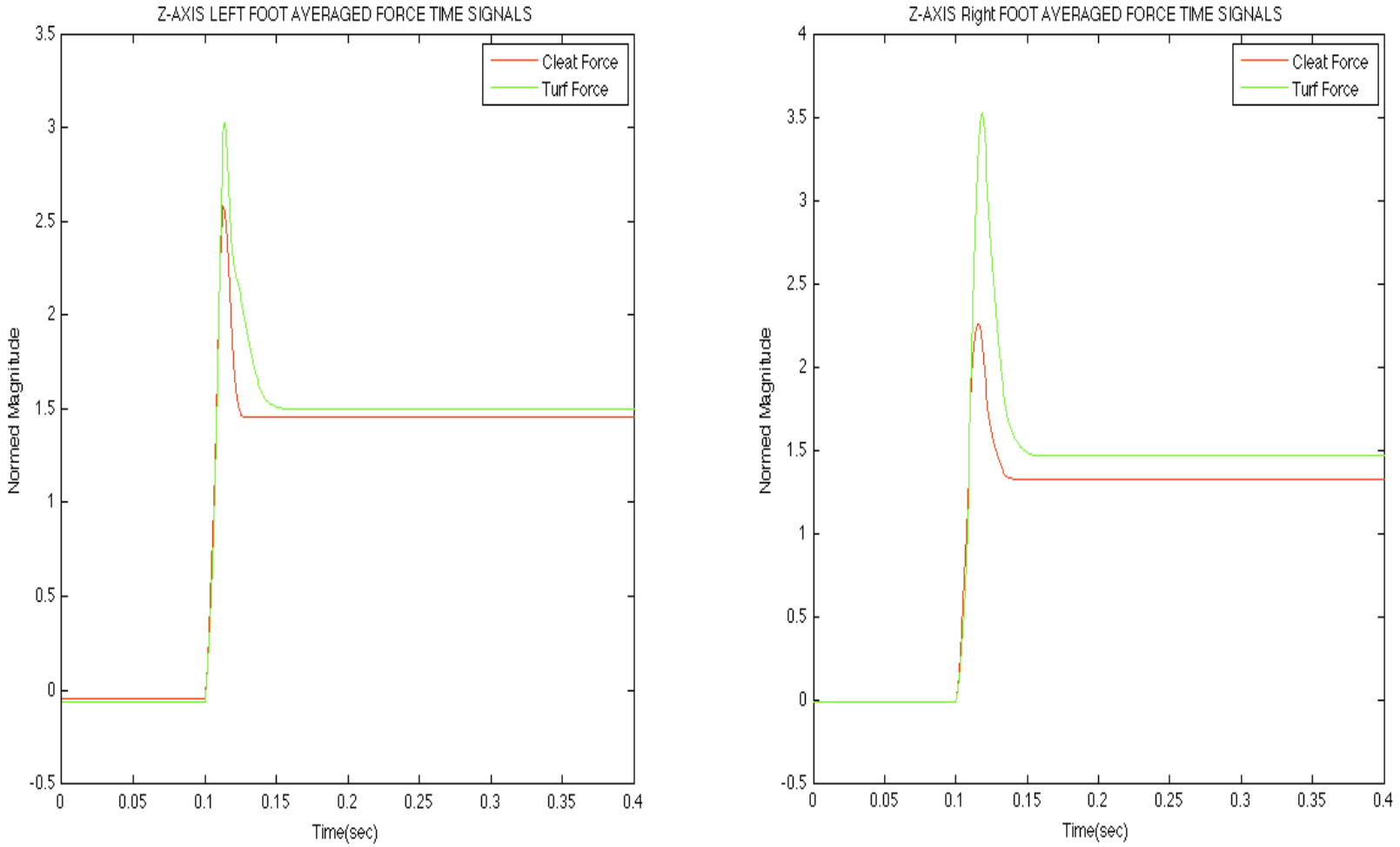

Figure 15. Z-Axis Averaged Force Signals of Cleat and Turf Shoe for Left and Right Foot (Not the Same Vertical Scale)

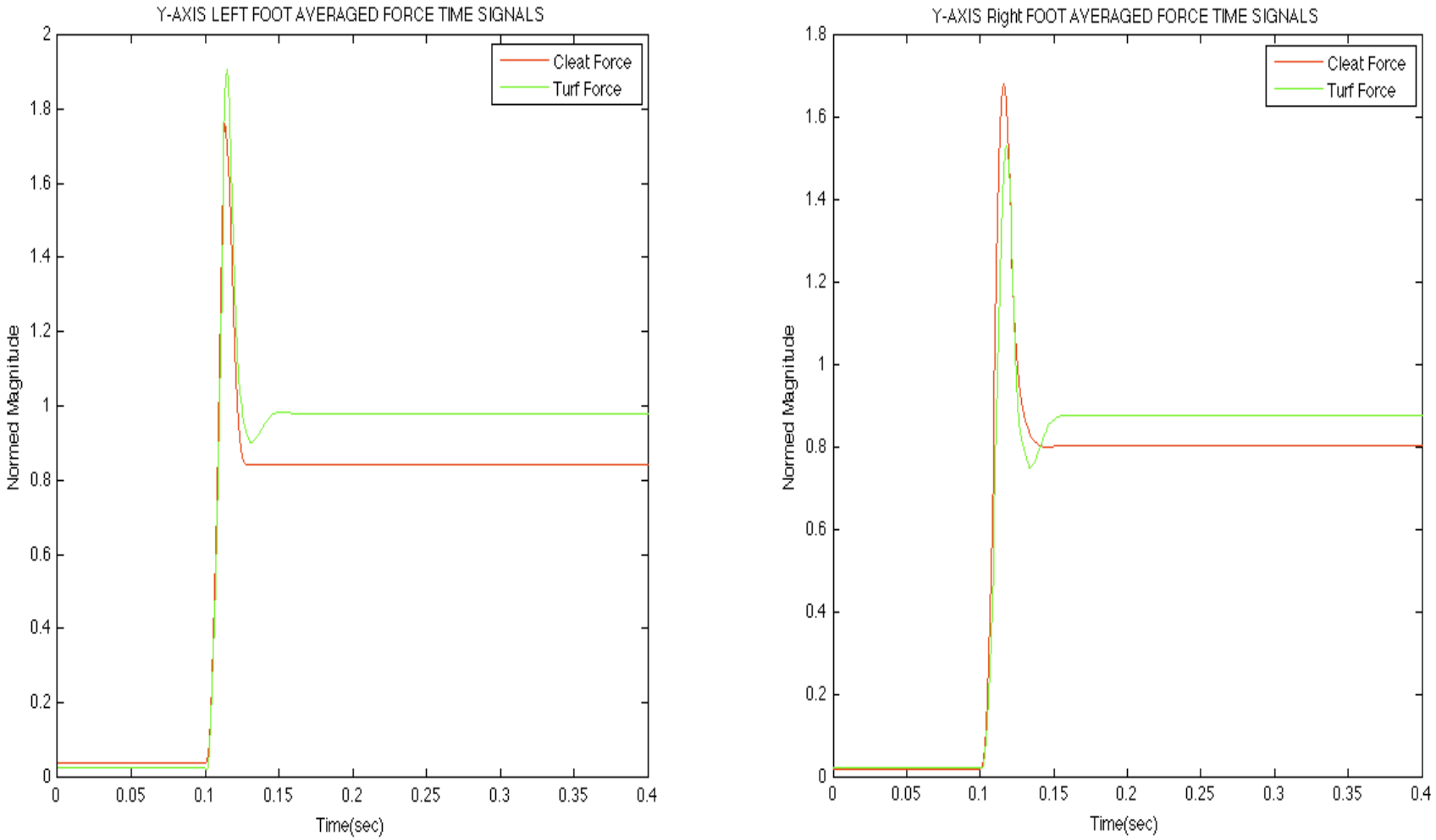

Figure 16. Y-Axis Averaged Force Signals of Cleat and Turf Shoe for Left and Right Foot (Not the Same Vertical Scale)

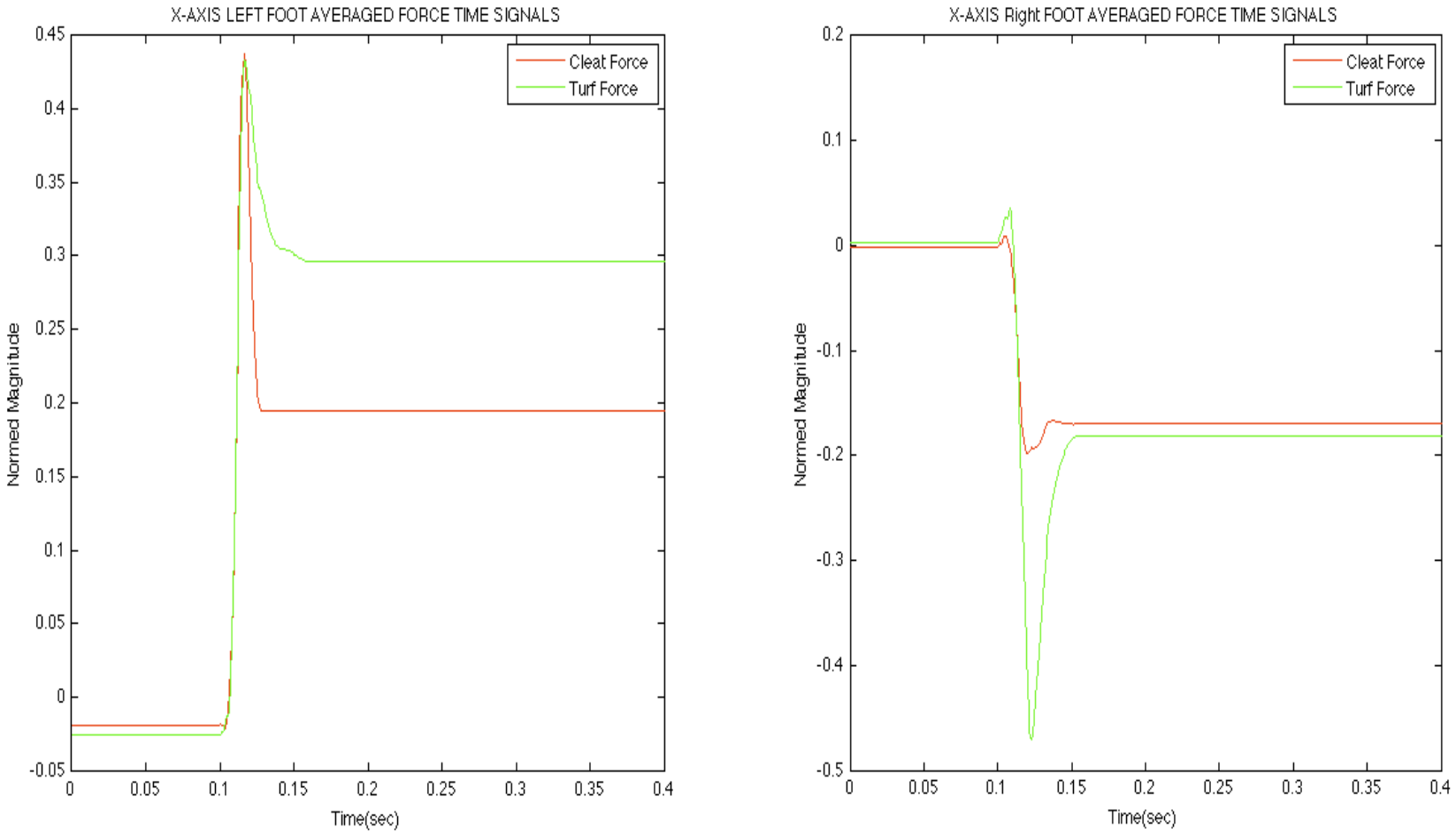

Figure 17. X-Axis Averaged Force Signals of Cleat and Turf Shoe for Left and Right Foot (Not the Same Vertical Scale)

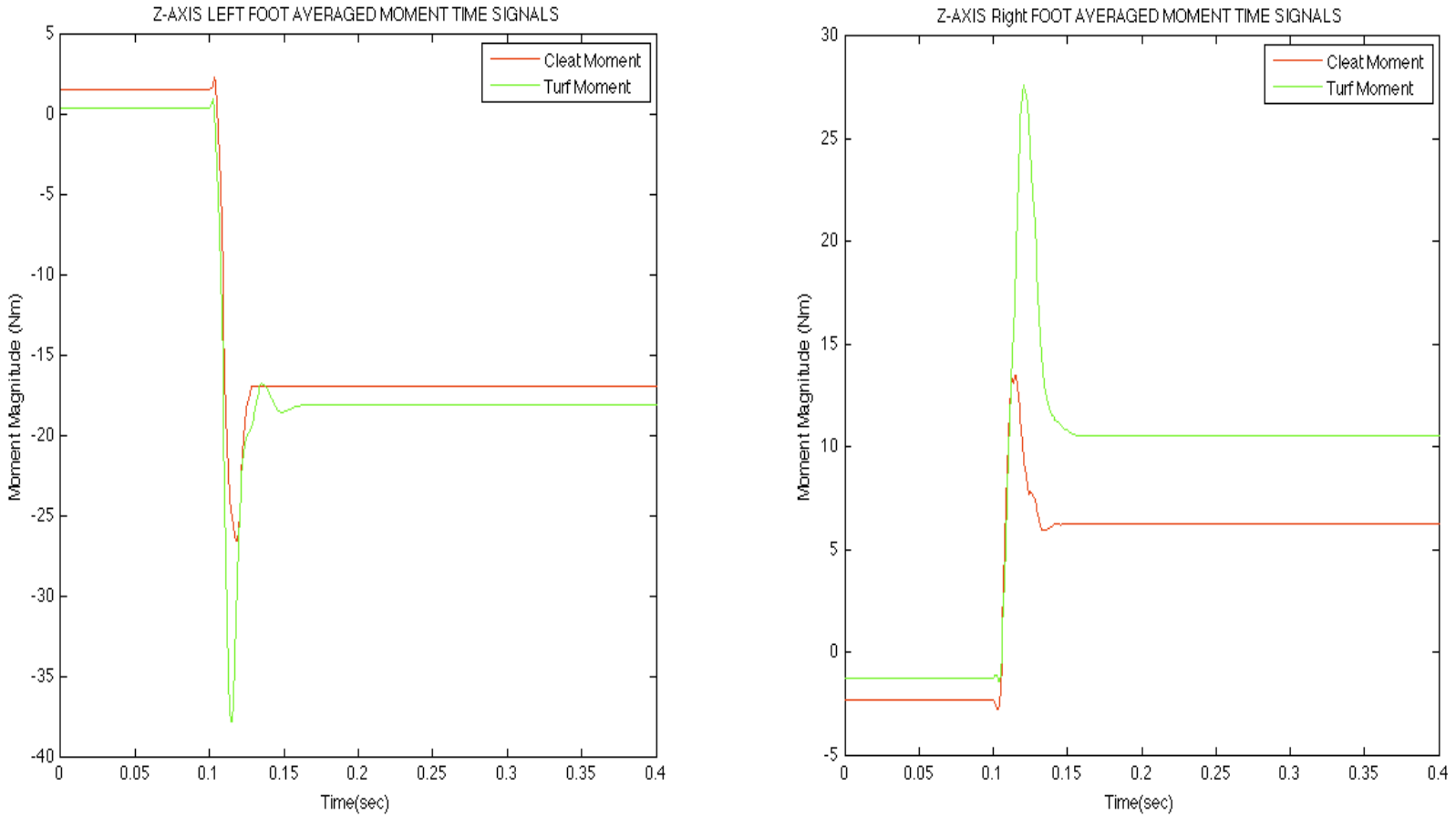

Figure 18. Z-Axis Averaged Moment Signals of Cleat and Turf Shoe for Left and Right Foot (Not the Same Vertical Scale)

Data Analysis

Each averaged signal was processed with the continuous wavelet transform using the complex Morlet wavelet as the mother wavelet. To take a spike in the time series into account, a 95% statistical confidence interval for the data was calculated according to the process describe by Ge [40]. Plus, to account for border effects a decorrelation calculation called the cone of influence (COI) was computed from a sample of the trials according to the procedure described by Torrence and Compo [34]. These statistics were used to ensure that the data to be analyzed is real and not a result of edge distortion from the wavelet transform or noise from the data acquisition process. Figure 19 on the next page illustrates an example of taking a sample force signal and plotting the results of the continuous wavelet transform and illustrating that the valid results are within a 95% confidence interval and the results outside of the COI, influenced by border effects of the signal, must not be considered when analyzing the data.

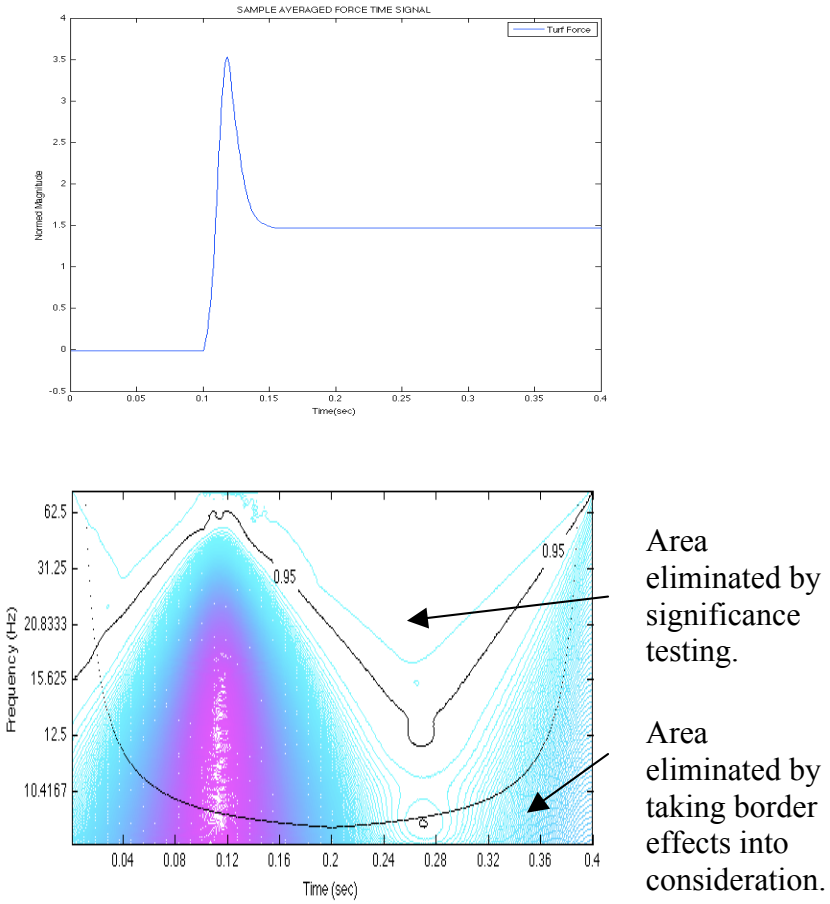

Figure 19. Wavelet Transform Example Showing Confidence Interval and COI.

Examining the region between the 95% confidence level and the COI, it was verified that the frequency content within the window of 11 to 60 Hz and 50 ms after the initial point of impact are valid analytical results for this data set.

To begin the process of comparing and contrasting the two signals the coherence between the two signals was computed, which Torrence and Compo refer to as the cross wavelet spectrum [34]. Cooper and Cowan refer to the same process as semblance analysis and have verified that "wavelets can be used to perform semblance analysis of time and spatial data series to display their correlations as a function of both scale (wavelength) and time (or position)" [41].

The coherence is computed by finding the arctangent between the real and imaginary parts of the dot product of the two signals in question. For this study, the arctangent2 command in Matlab was used to provide a unique value between –pi and +pi to discern which quadrant the coherence occurs and for ease of viewing, the values plotted were divided by pi to provide a spectrum between -1 and +1, where a value of zero represents the greatest difference between the two signals. With the atan2 function, ”there is also a discontinuity where –pi and +pi describe the same series of points along the negative X axis (between quadrants 2 and 3)” [42]. In this study, the discontinuity is acceptable because it is far from the area of interest.

Shown in Figure 20 is an example of CWT coherence plots, along with its corresponding coherence phase plot. The plot shows the original cleat and non-cleated turf shoe signals for a given axis (the Z-axis in this case), along with the CWT of each signal. In this case, the coherence plot shows that the signals match in magnitude between 11 Hz and 20 Hz range, but their phase dissimilarity shows up in the coherence phase plot where zero is represented by the light green color. The complete results for each GRF and the vertical moment of both the cleated and non-cleated turf signals of the left and right foot are provided in the results section of this document.

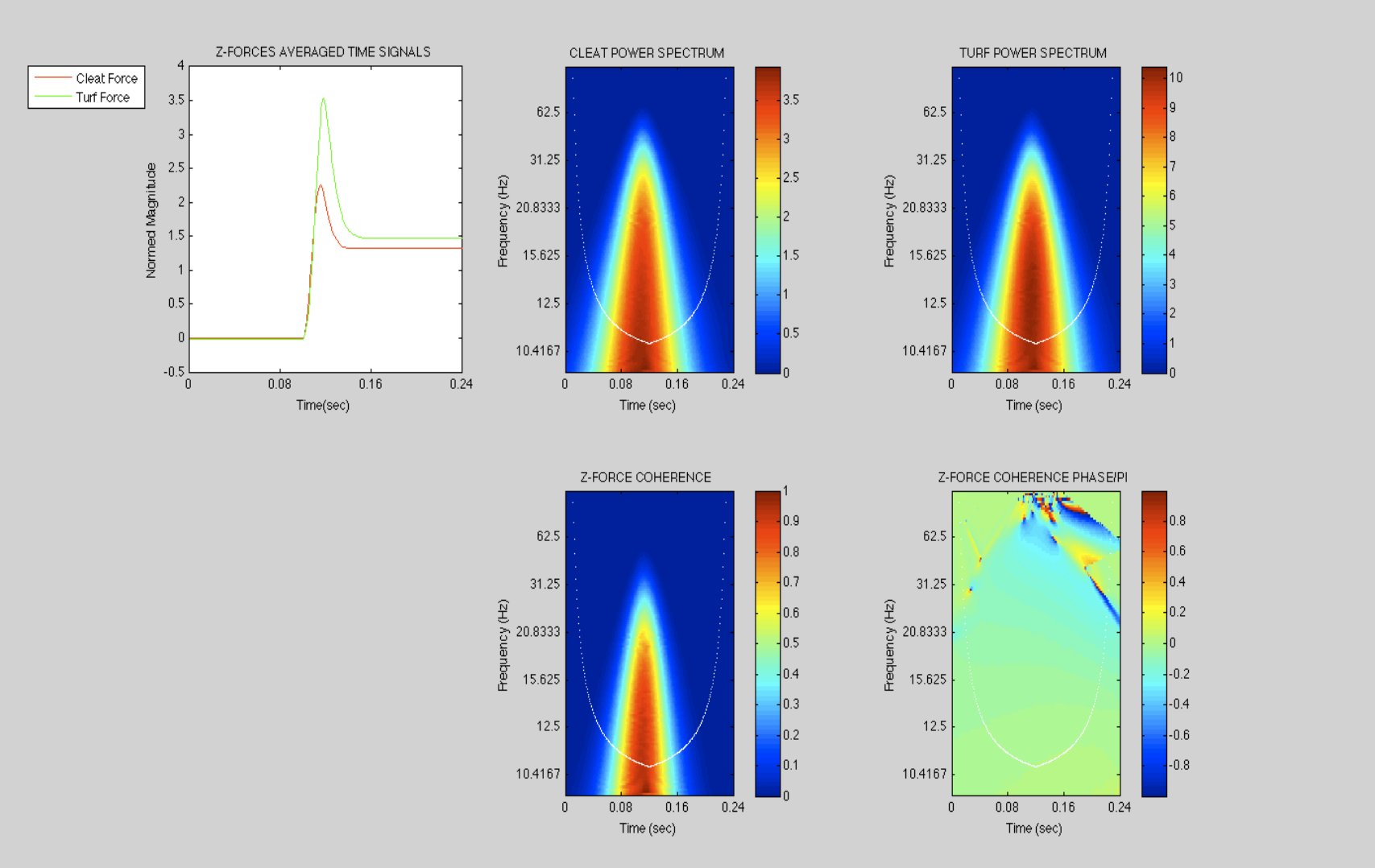

Figure 20. Example Result of CWT Coherence and Coherence Phase between Two Signals (Right Foot GRF in the Z Direction)

To elucidate the similarities and differences between the two signals, slices of both CWT plots at specific frequencies can be taken and plotted together. In this study, a slice at 11 Hz was taken, then 15 Hz, and so on at 5 Hz intervals, to end at 65 Hz. As an example, Figure 21 below shows a slice of the vertical force for the right foot at 25 Hz for the two signals used to produce the coherence plots in Figure 20.

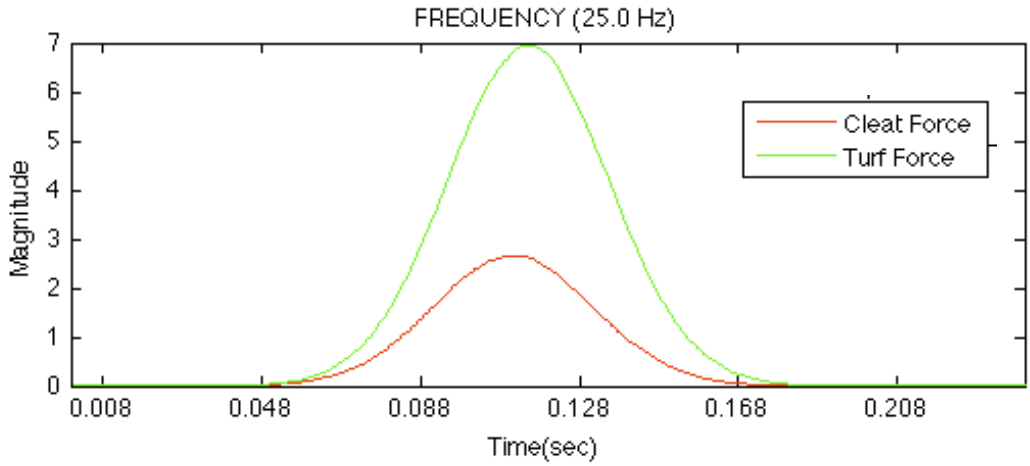

Figure 21. Example of two CWT plots sliced at 25 Hz.

The complete results at particular frequencies (approximately 5 Hz intervals) for each GRF and the vertical moment of both the cleated and non-cleated turf signals of the left and right foot are provided in the results section of this document.

The final step to analyzing the data was to find the percent difference between the maximum values of the wavelet slices at each specific frequency to quantify the similarity or difference between the two signals, and then to plot the results for each GRF and for the vertical moment force.

RESULTS

From a previous study using the same data set, the mean peak vertical GRF for the left and right foot for both the cleated and non-cleated turf shoe trails were calculated and a statistical t-test was performed [43]. Table 2 is a summary of the statistical results for the straight ahead (center) cut and run test trials.

Table 2. Statistical Comparison of the Mean Peak Vertical Ground Reaction Forces

	Left Leg	**Right Leg**
Cleated (N)	1836.5	2118.4
Standard Deviation	649	617
Non-Cleated (N)	2122.6	2479.2
Standard Deviation	251	608
Percent Difference	15.6	17
T-Test	0.20	0.31

The t-test value for both the left and right legs are low; however, they are both above 0.05 indicating they are not significantly different.

Looking at the anterior posterior (Y-Force) data for the left and right foot for both the cleated and non-cleated turf shoe trials, it was possible to determine which foot provided the primary push off force necessary to create forward momentum. On average when the subjects wore the cleated shoe there was little difference between the use of the left and right foot for push off (45.8 versus 54.2 respectively); however, for the non-

cleated turf shoe trials, the subjects used their right foot to push off 79.2 percent of the time.

This difference can be seen in the average vertical force of impact when comparing the left and right foot for both the cleated and non-cleated subjects. On average, the cleated subjects had a normalized vertical impact force of 2.26 for the left foot and 2.59 for the right foot. In comparison, for the non-cleated turf shoe, the averaged normalized vertical impact force was 3.03 for the left foot, and 3.53 for the right foot. Thus, both vertical impact signals are stronger for the non-cleated turf shoe regardless of being the left or right foot when contrasted with the cleated shoe, and the right foot received the dominant impact force in anticipation of being the dominant push off foot.

The following pages provide the complete CWT and coherence plot results for each GRF and the vertical moment of both the cleated and non-cleated turf signals of the left and right foot. Following each result, slices at particular frequencies at approximate 5 Hz intervals between 10 Hz and 65 Hz, are also provided, which can be used to visually compare and contrast the magnitude of the frequency for both types of shoes.

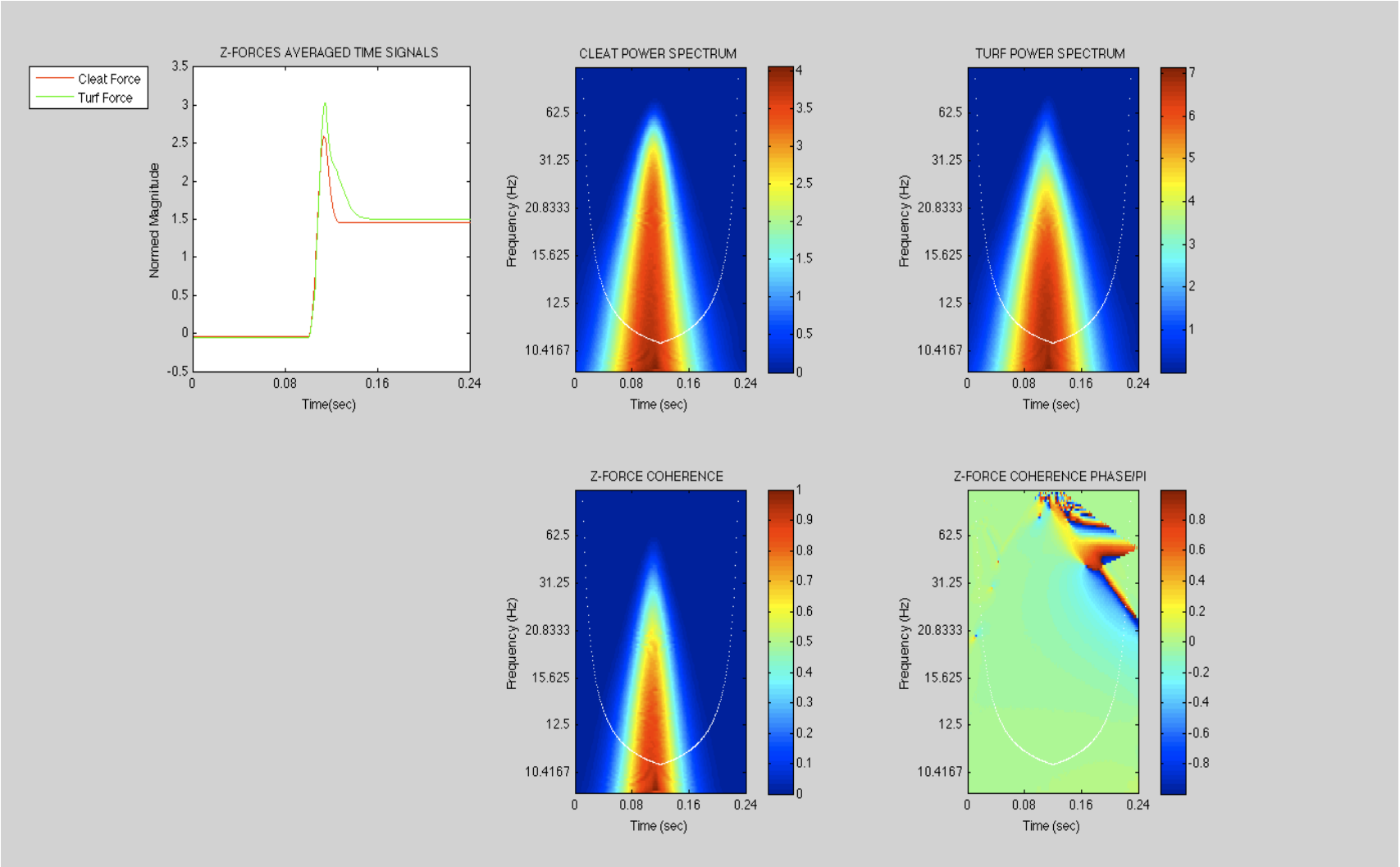

Figure 22. Left Foot Ground Reaction Force in the Z Direction with CWT Analysis

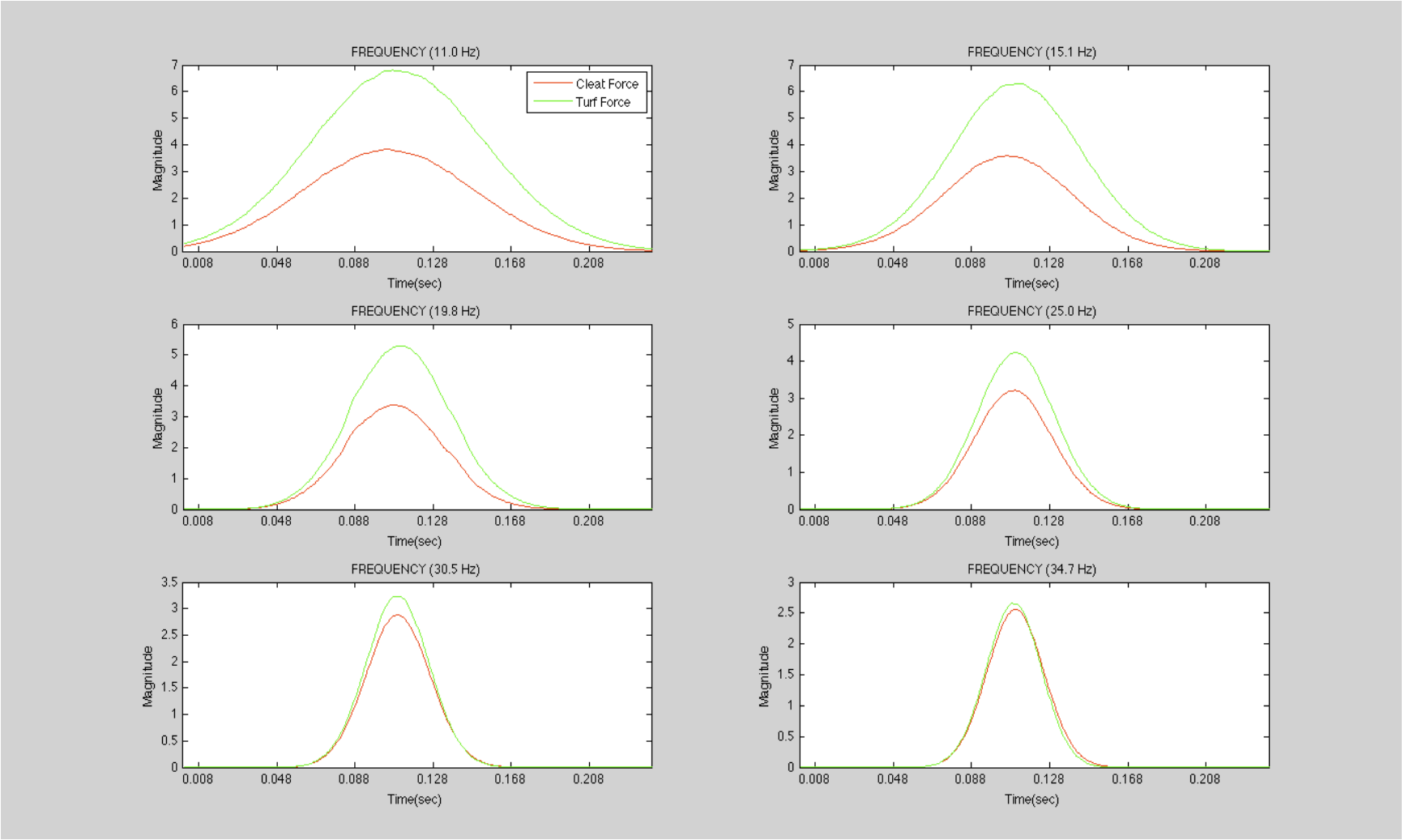

Figure 23. Left Foot Z-Force Cross-Sections of Power Spectrum from 11 Hz to 35 Hz

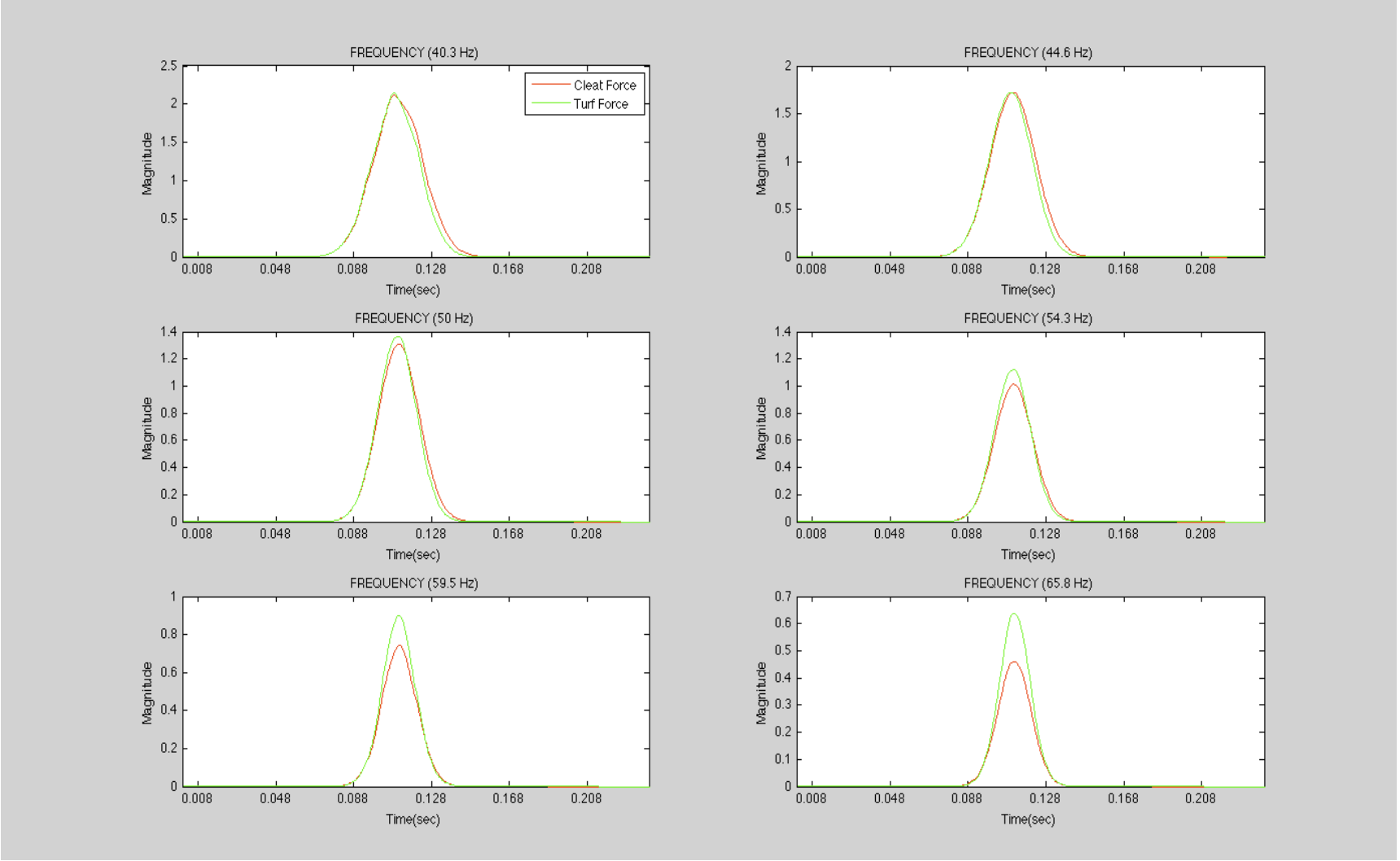

Figure 24. Left Foot Z-Force Cross-Sections of Power Spectrum from 40 Hz to 65 Hz.

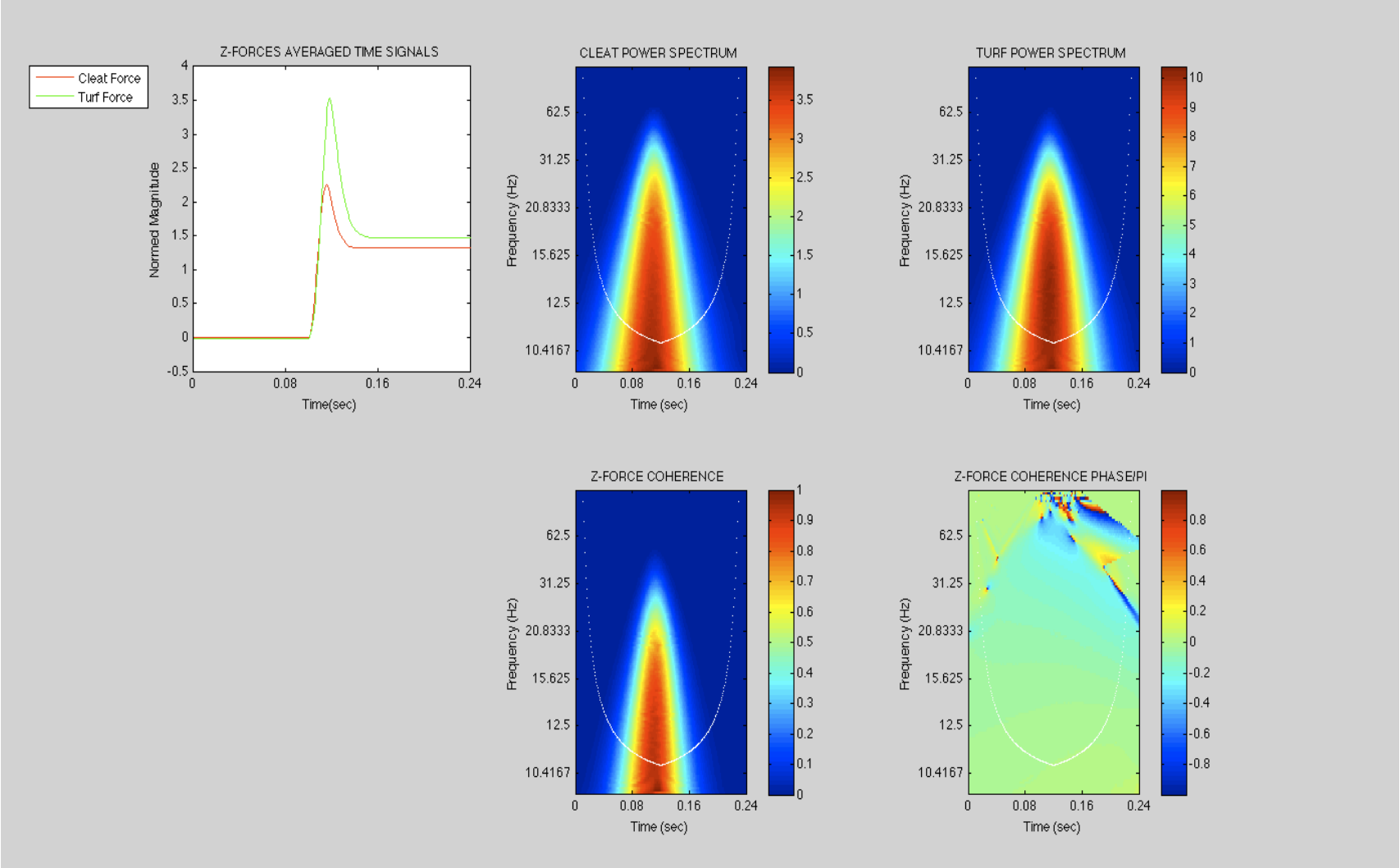

Figure 25. Right Foot Ground Reaction Force in the Z Direction with CWT Analysis

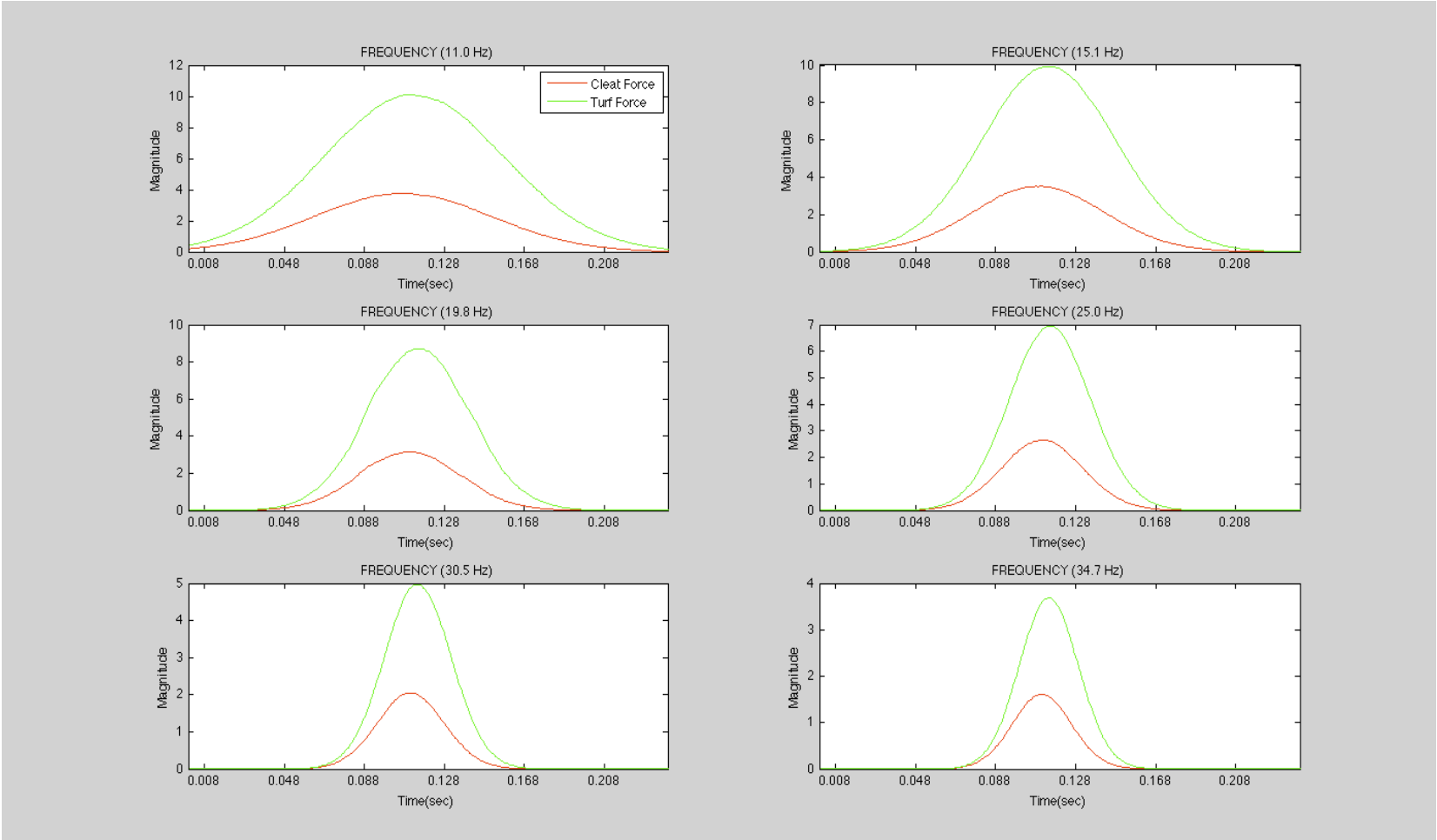

Figure 26. Right Foot Z-Force Cross-Sections of Power Spectrum from 11 Hz to 35 Hz.

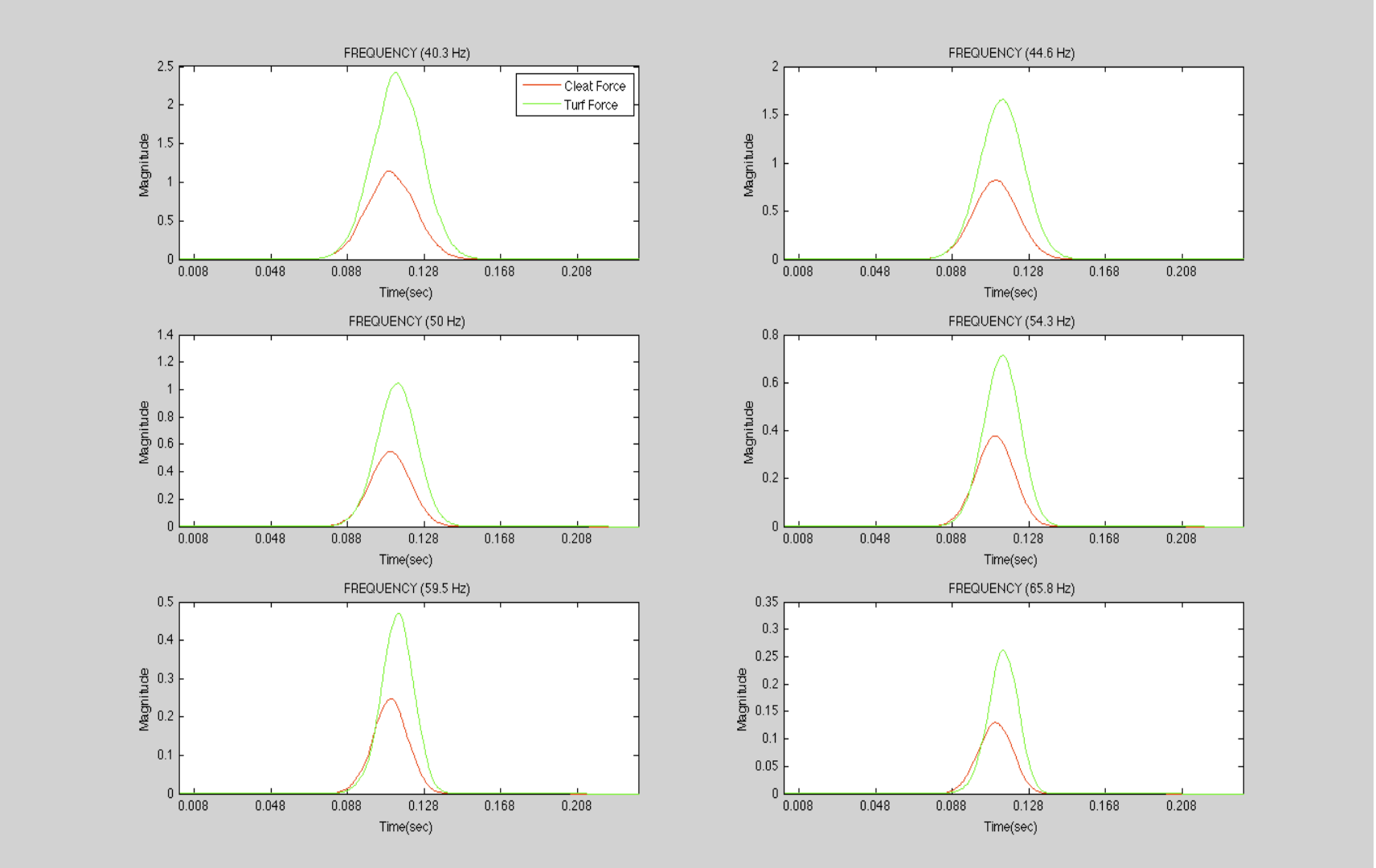

Figure 27. Right Foot Z-Force Cross-Sections of Power Spectrum from 40 Hz to 65 Hz.

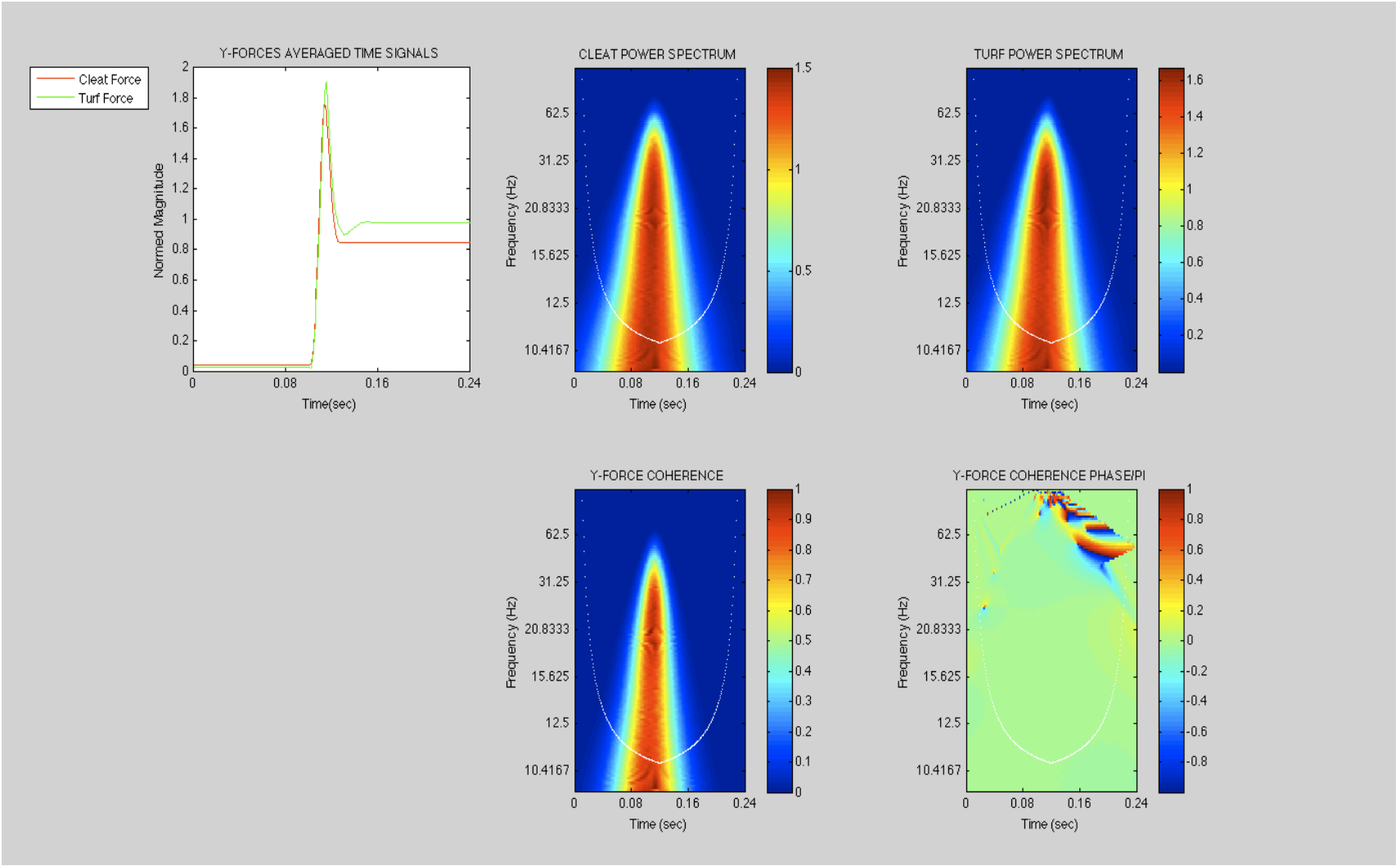

Figure 28. Left Foot Ground Reaction Force in the Y Direction with CWT Analysis

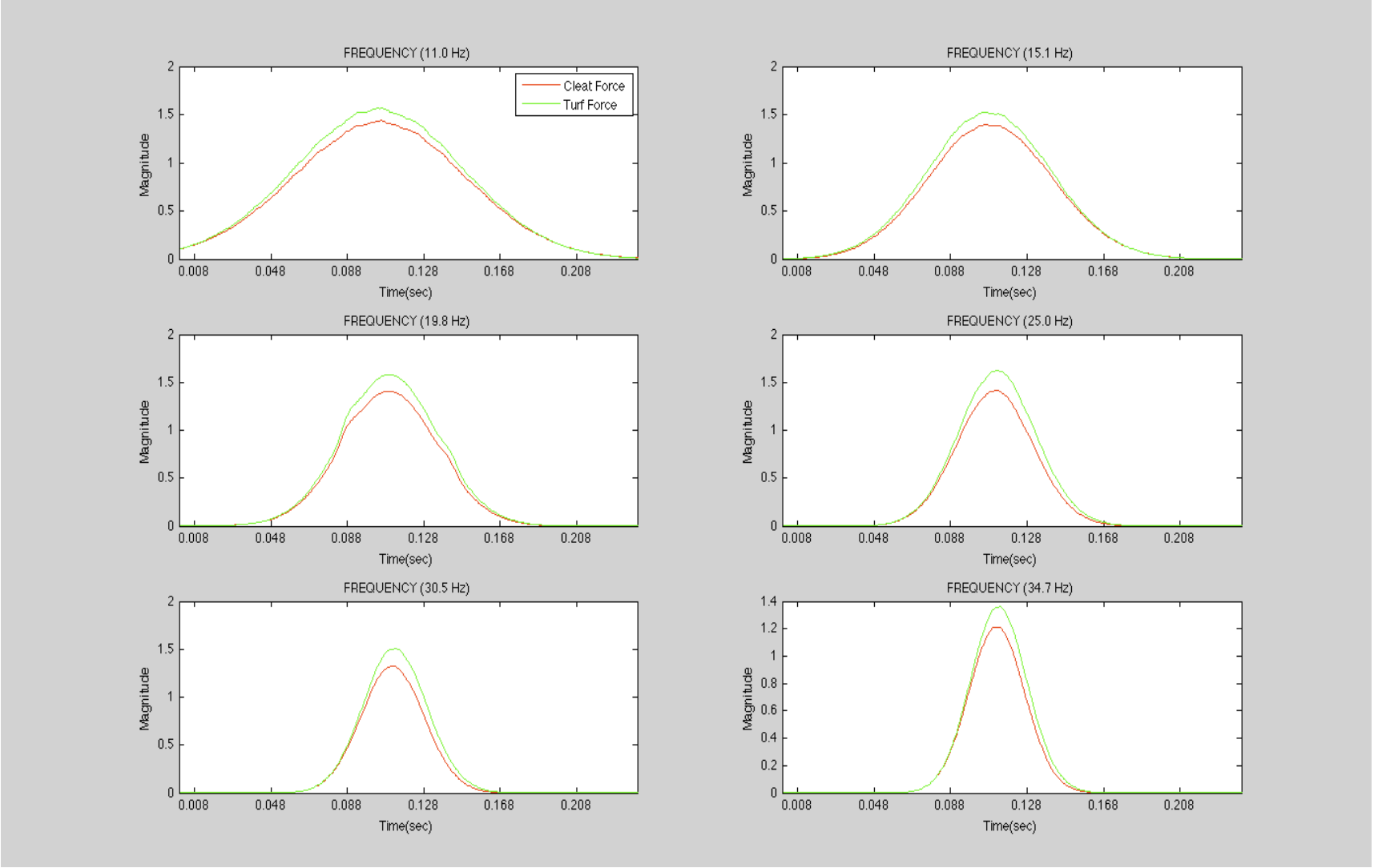

Figure 29. Left Foot Y-Force Cross-Sections of Power Spectrum from 11 Hz to 35 Hz.

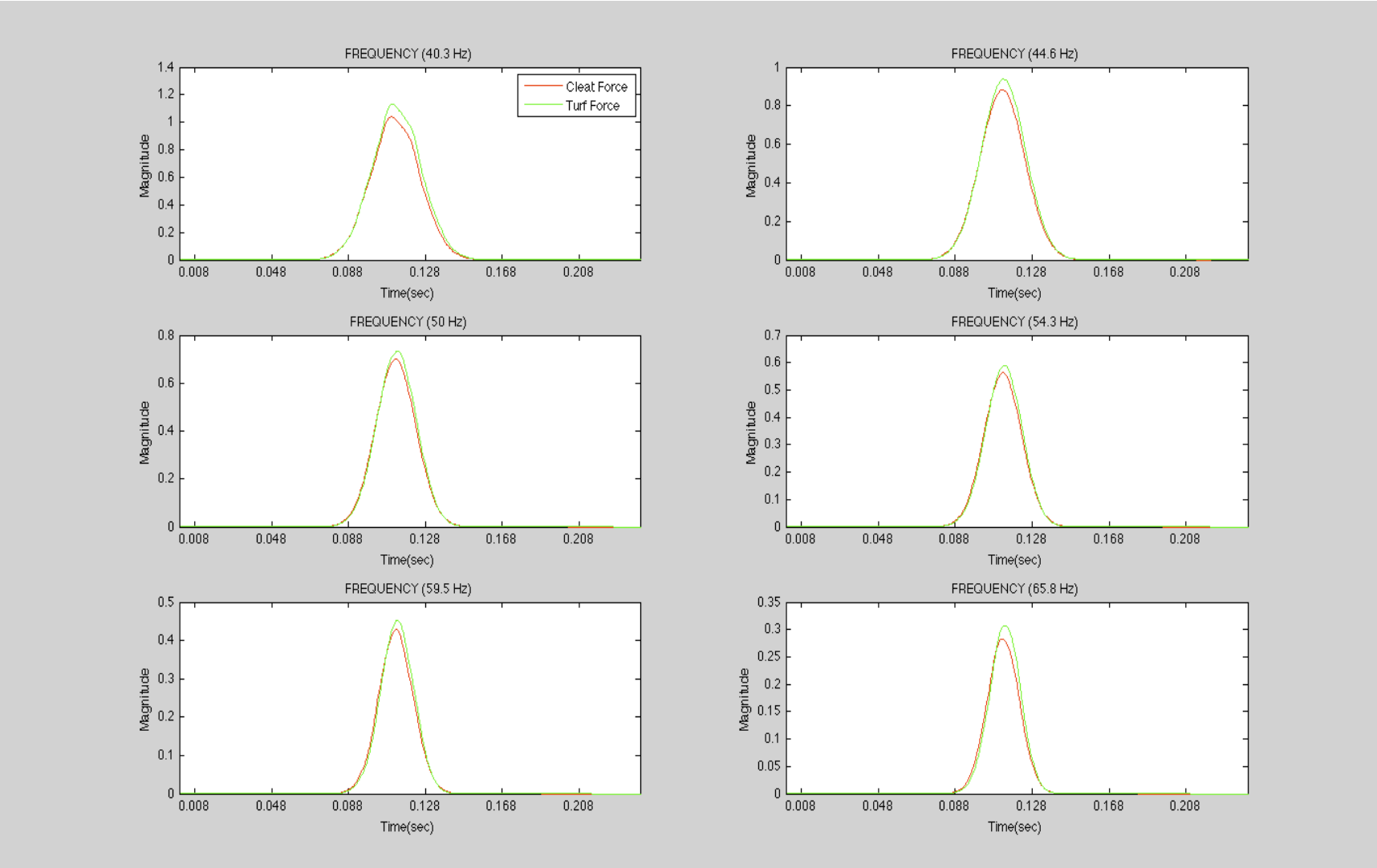

Figure 30. Left Foot Y-Force Cross-Sections of Power Spectrum from 40 Hz to 65 Hz.

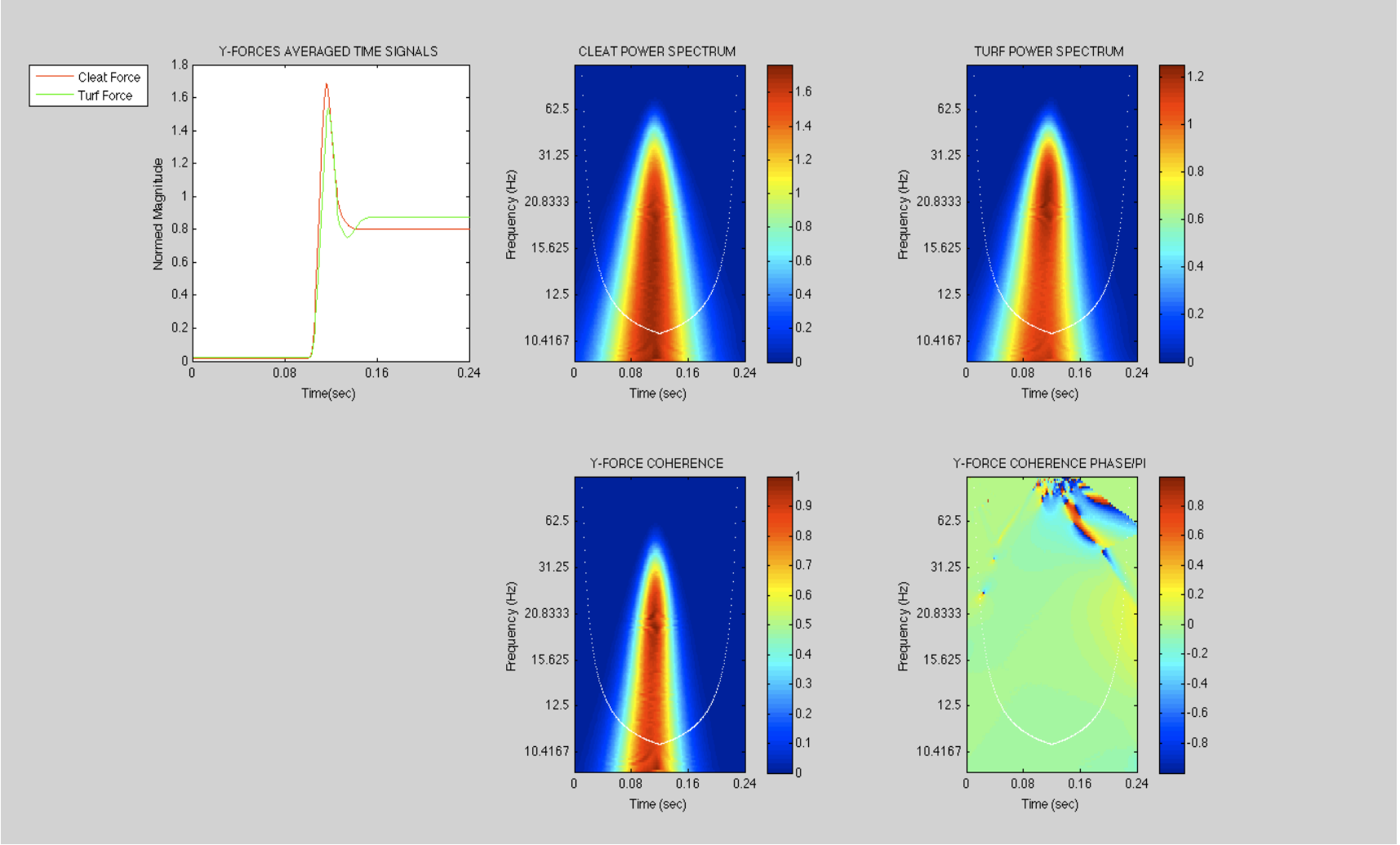

Figure 31. Right Foot Ground Reaction Force in the Y Direction with CWT Analysis

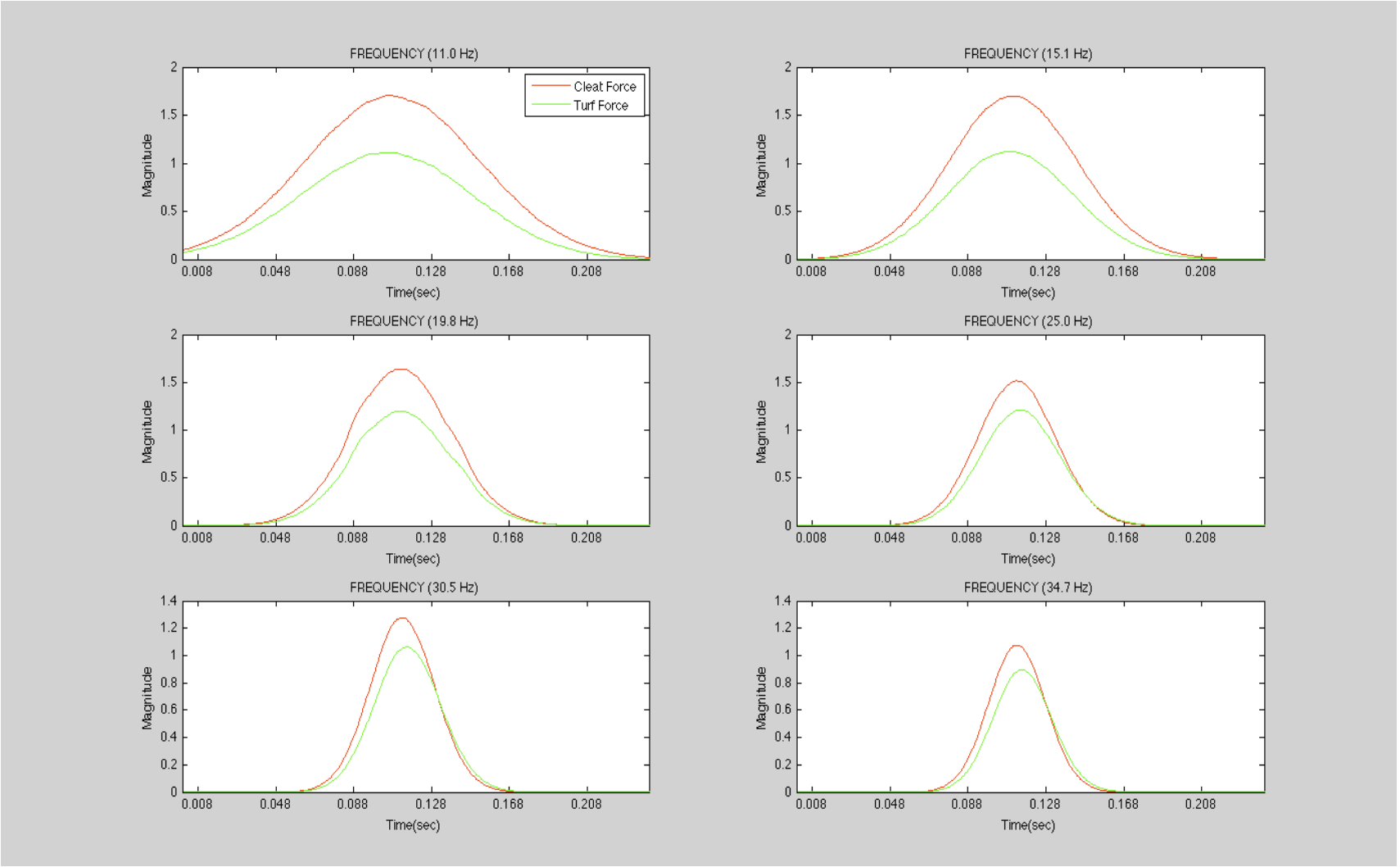

Figure 32. Right Foot Y-Force Cross-Sections of Power Spectrum from 11 Hz to 35 Hz.

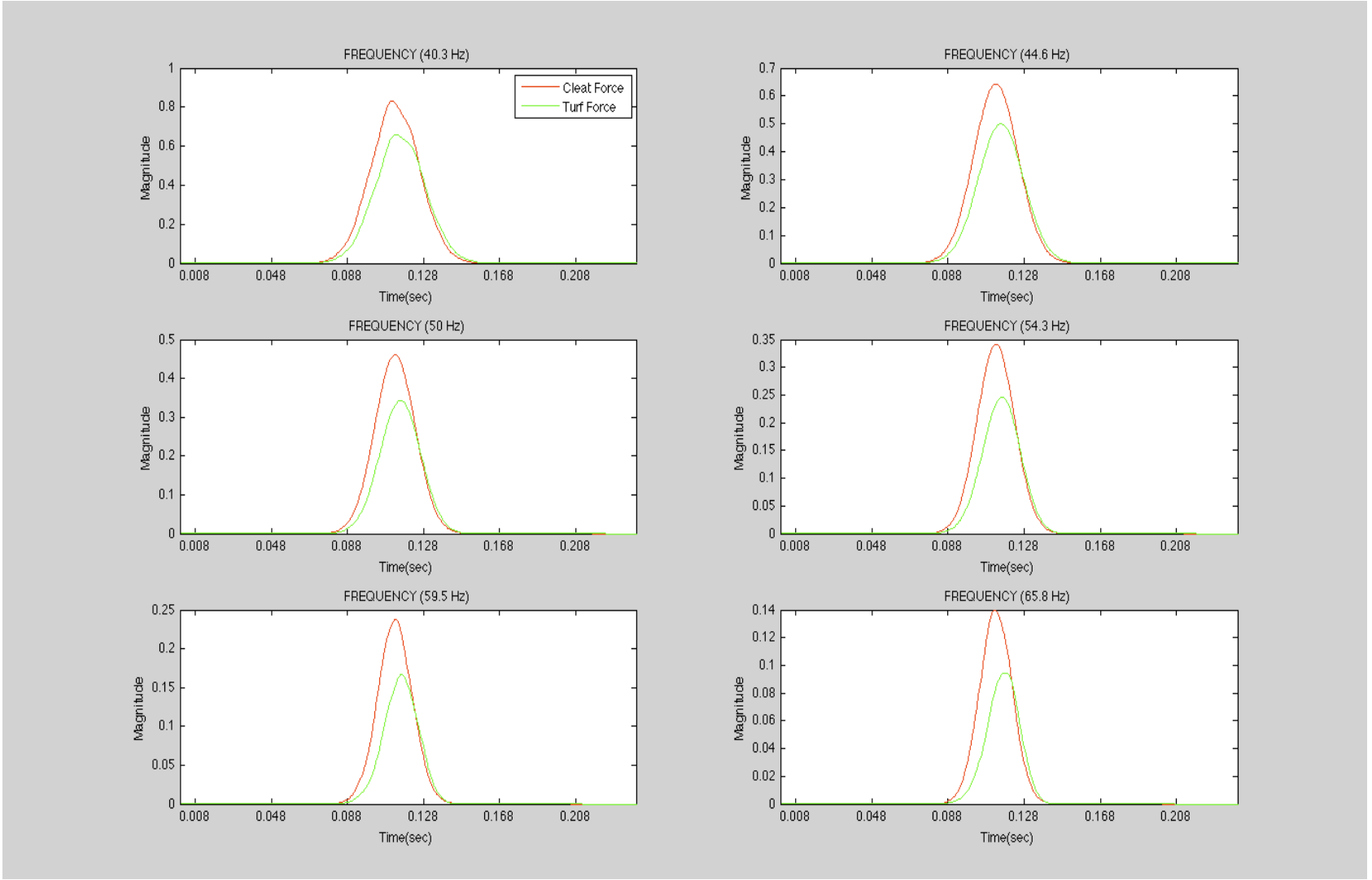

Figure 33. Right Foot Y-Force Cross-Sections of Power Spectrum from 40 Hz to 65 Hz.

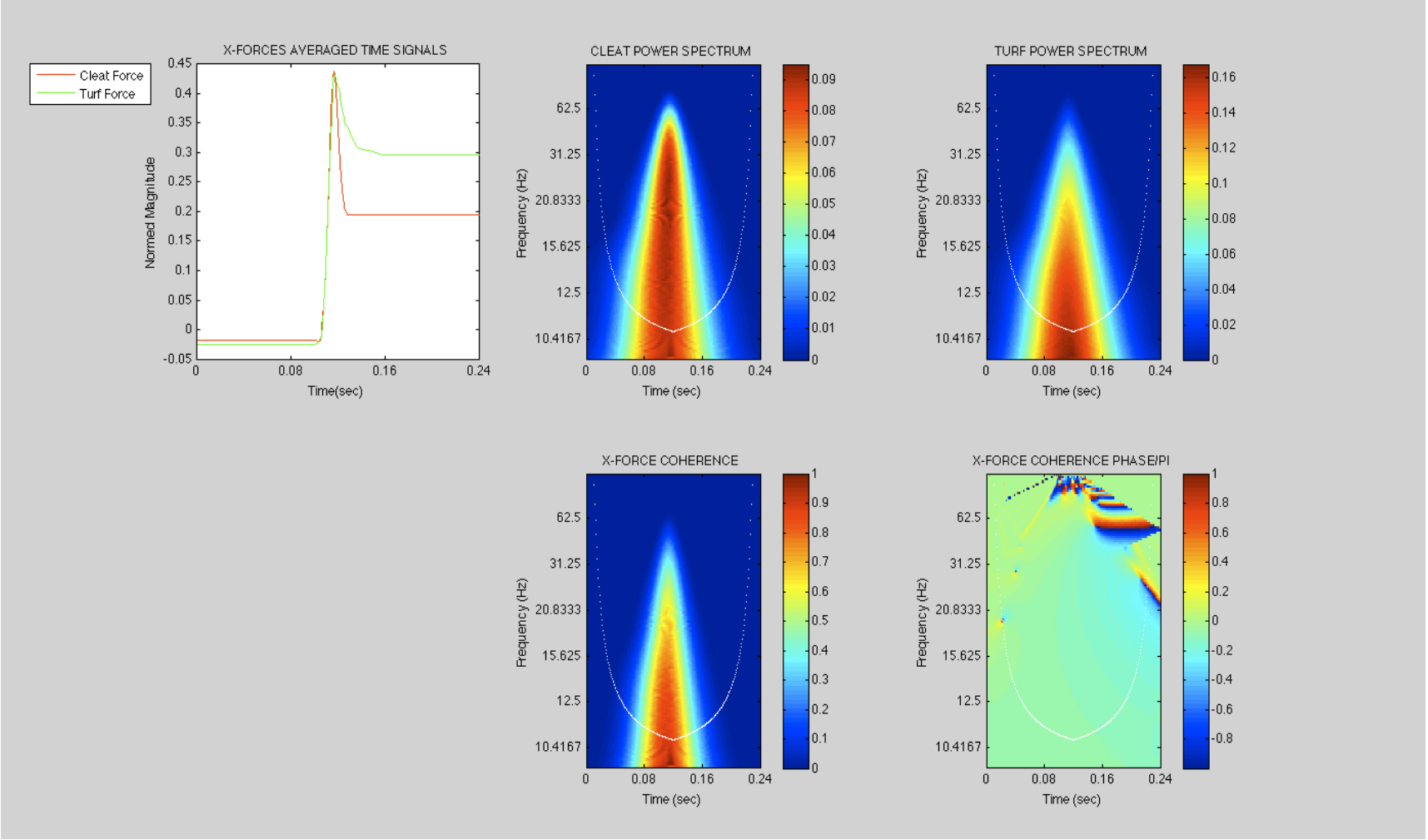

Figure 34. Left Foot Ground Reaction Force in the X Direction with CWT Analysis

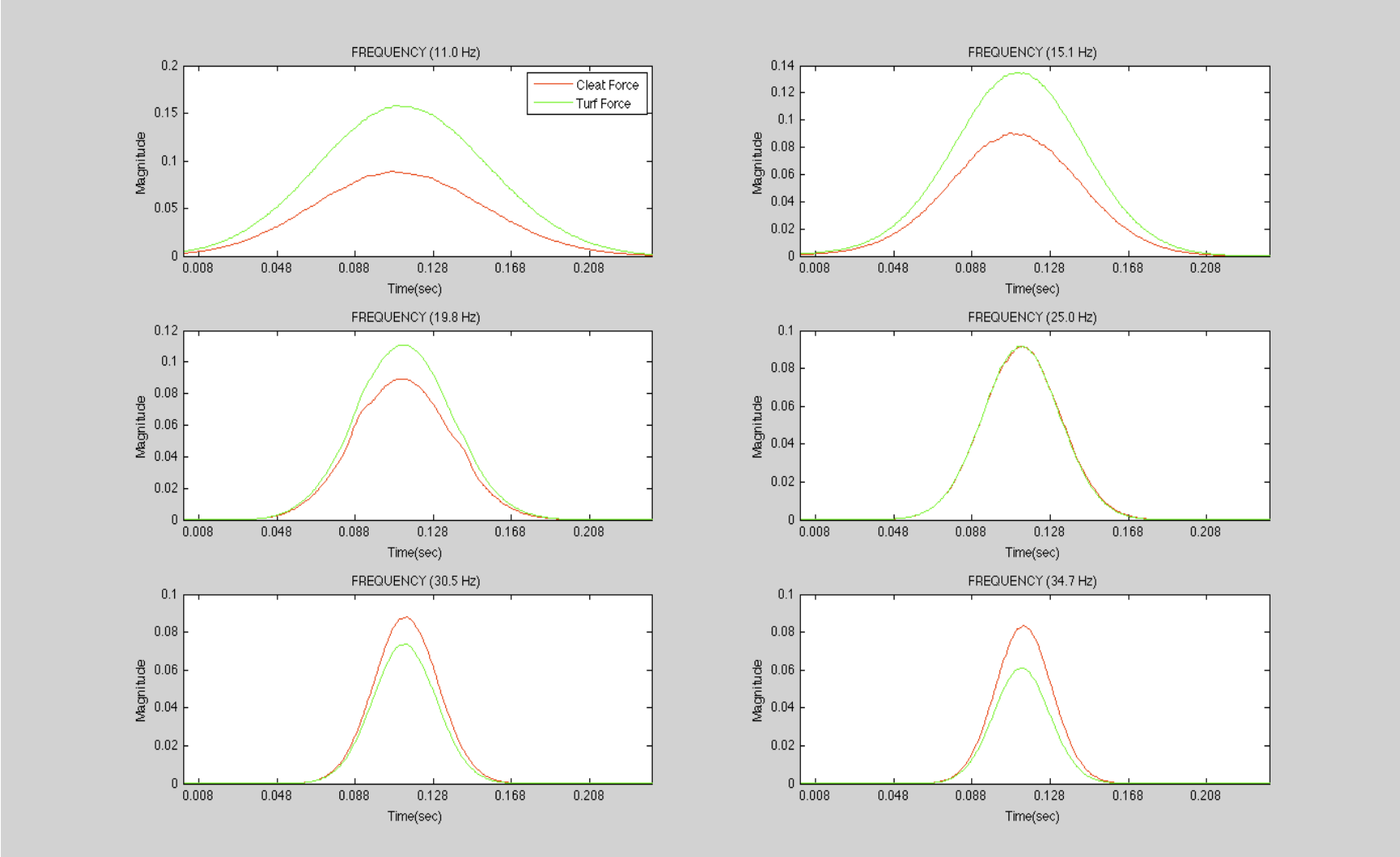

Figure 35. Left Foot X-Force Cross-Sections of Power Spectrum from 11 Hz to 35 Hz.

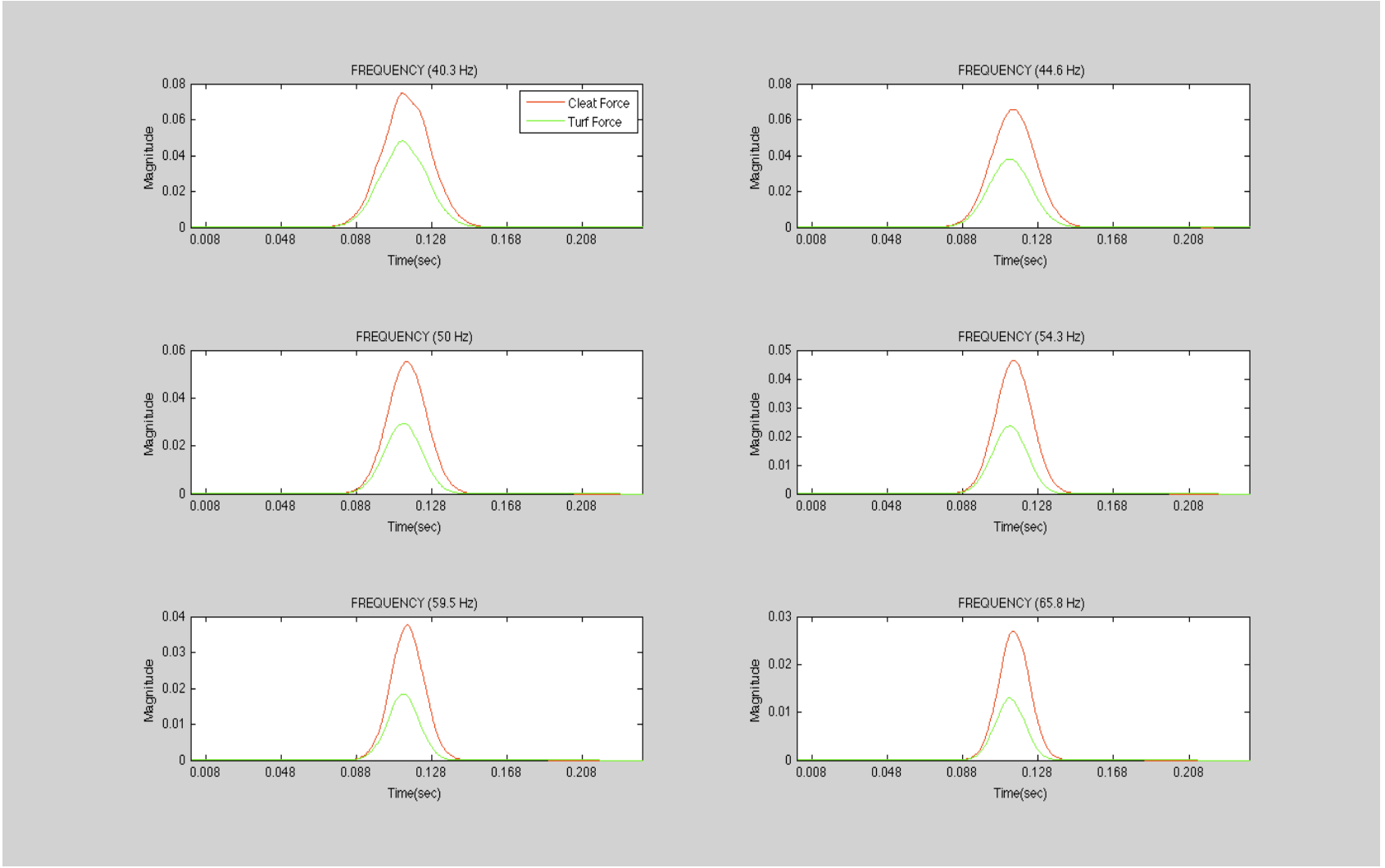

Figure 36. Left Foot X-Force Cross-Sections of Power Spectrum from 40 Hz to 65 Hz.

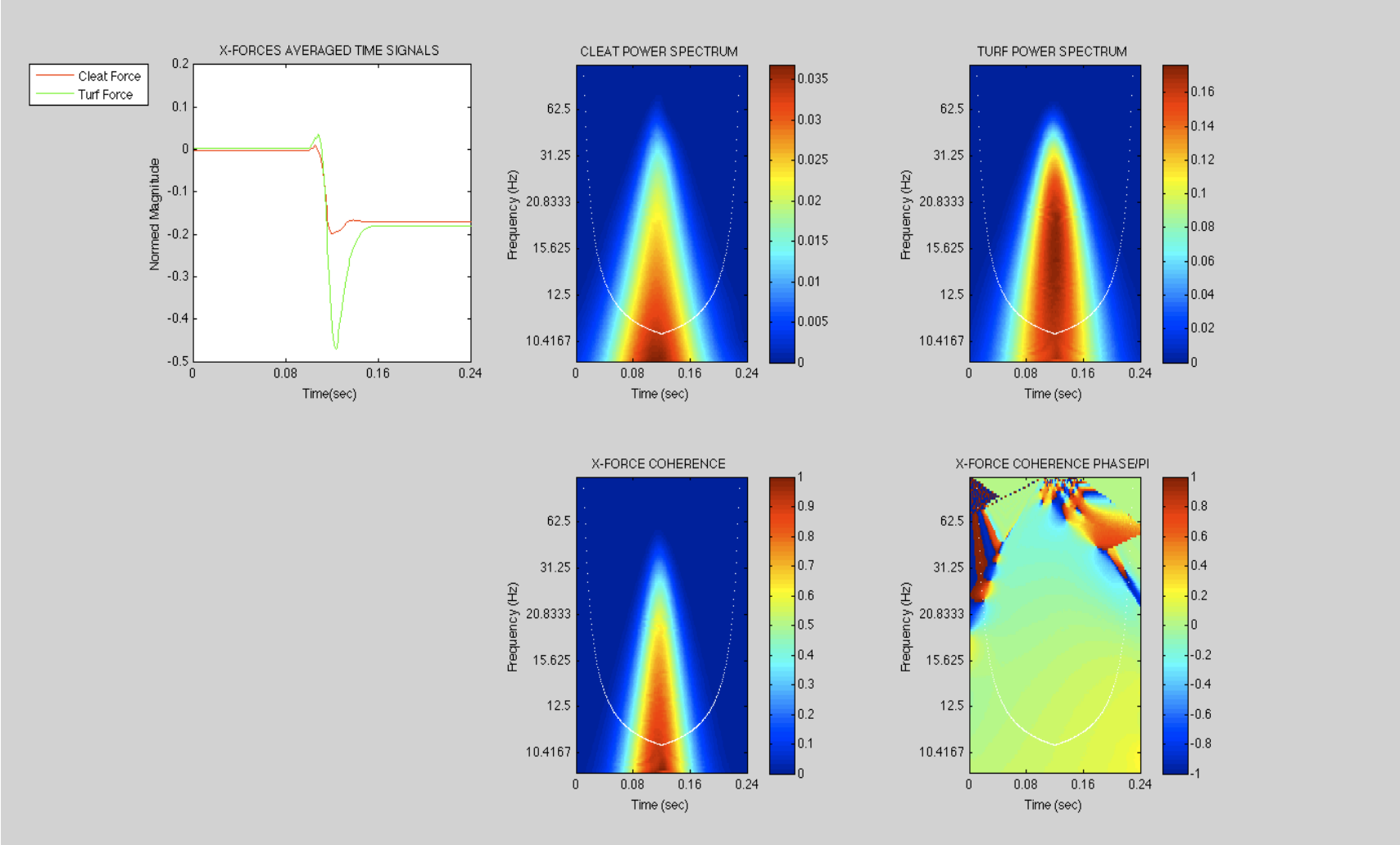

Figure 37. Right Foot Ground Reaction Force in the X Direction with CWT Analysis

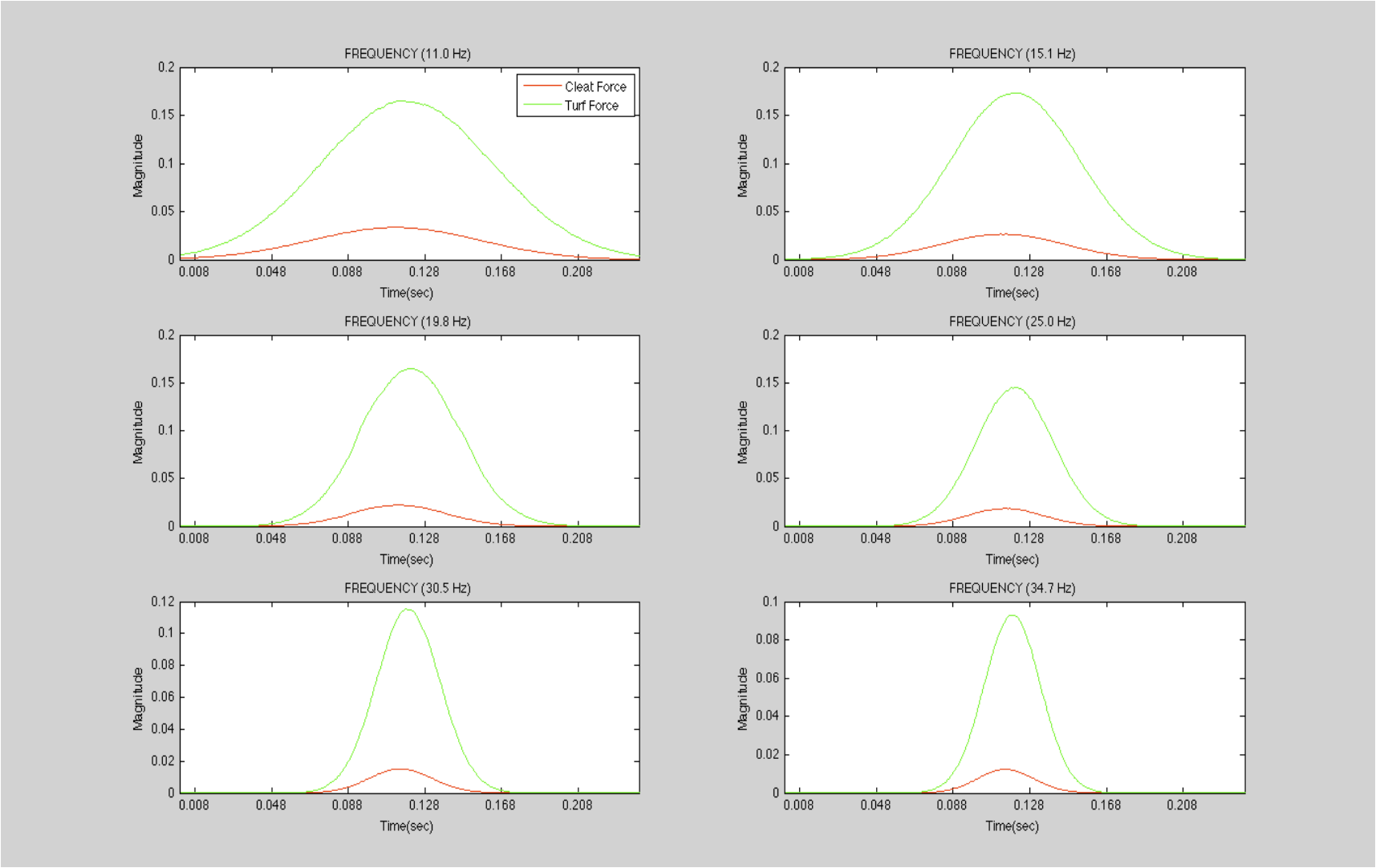

Figure 38. Right Foot X-Force Cross-Sections of Power Spectrum from 11 Hz to 35 Hz.

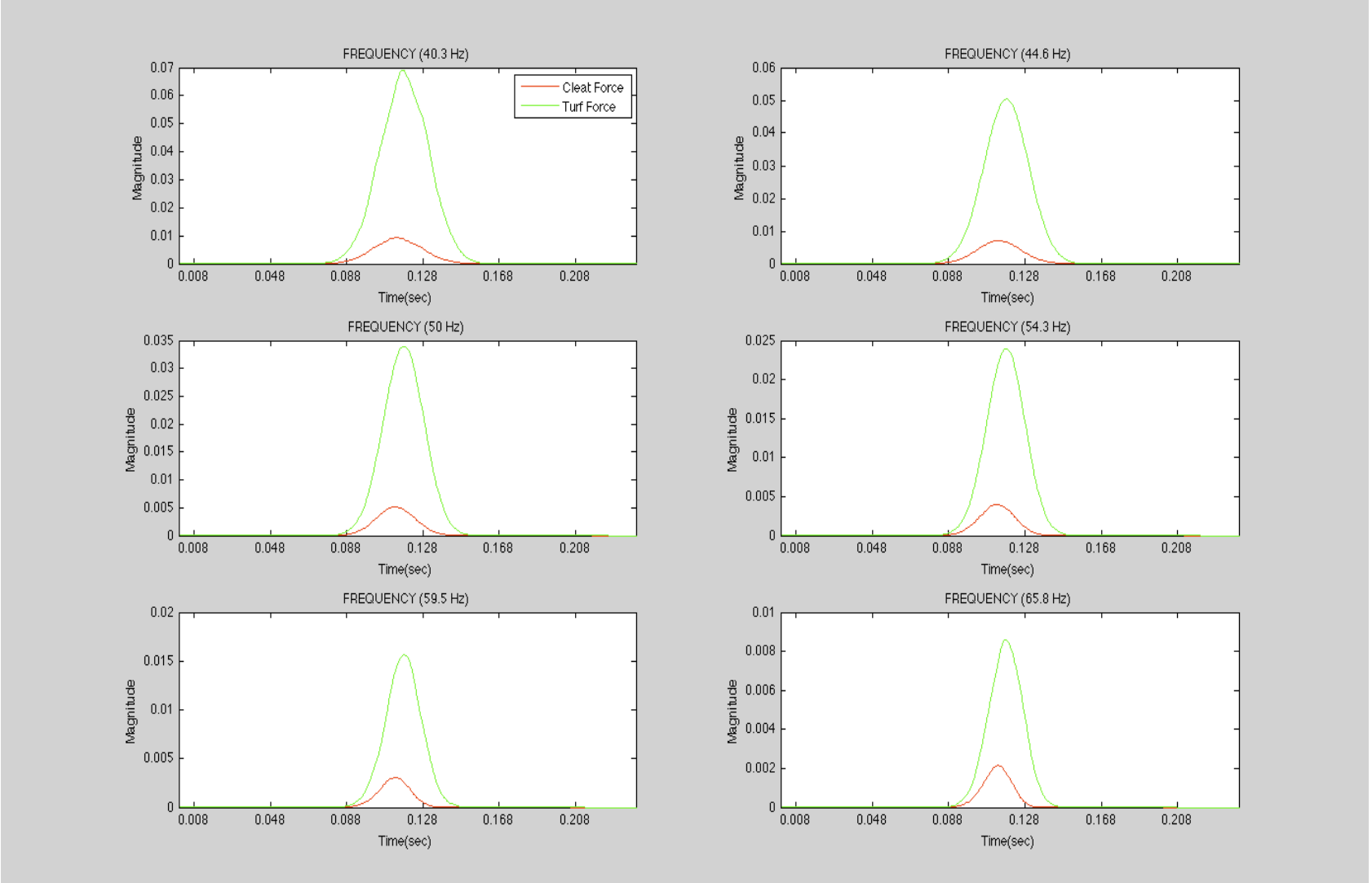

Figure 39. Right Foot X-Force Cross-Sections of Power Spectrum from 40 Hz to 65 Hz.

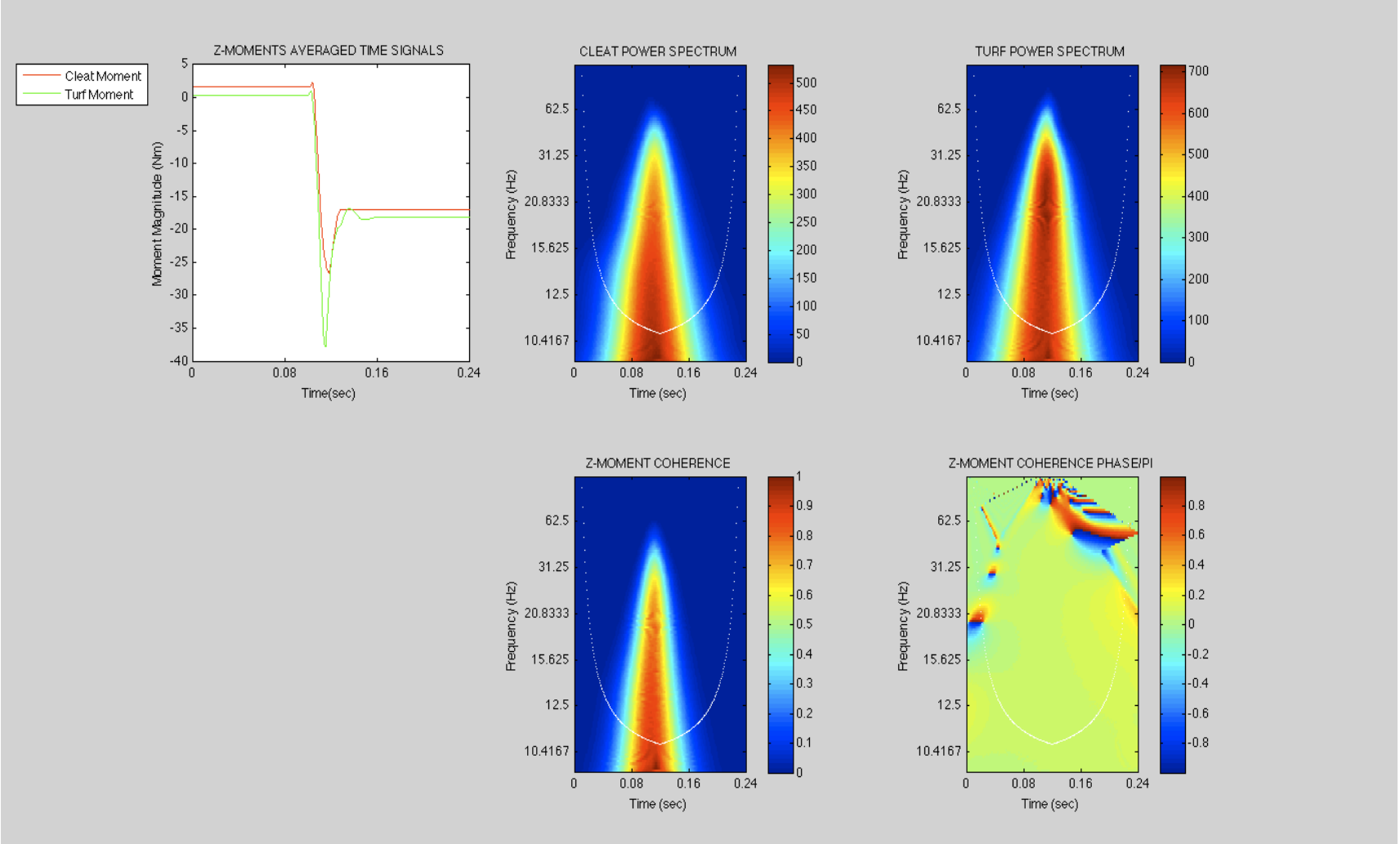

Figure 40. Left Foot Ground Reaction Moment in the Z Direction with CWT Analysis

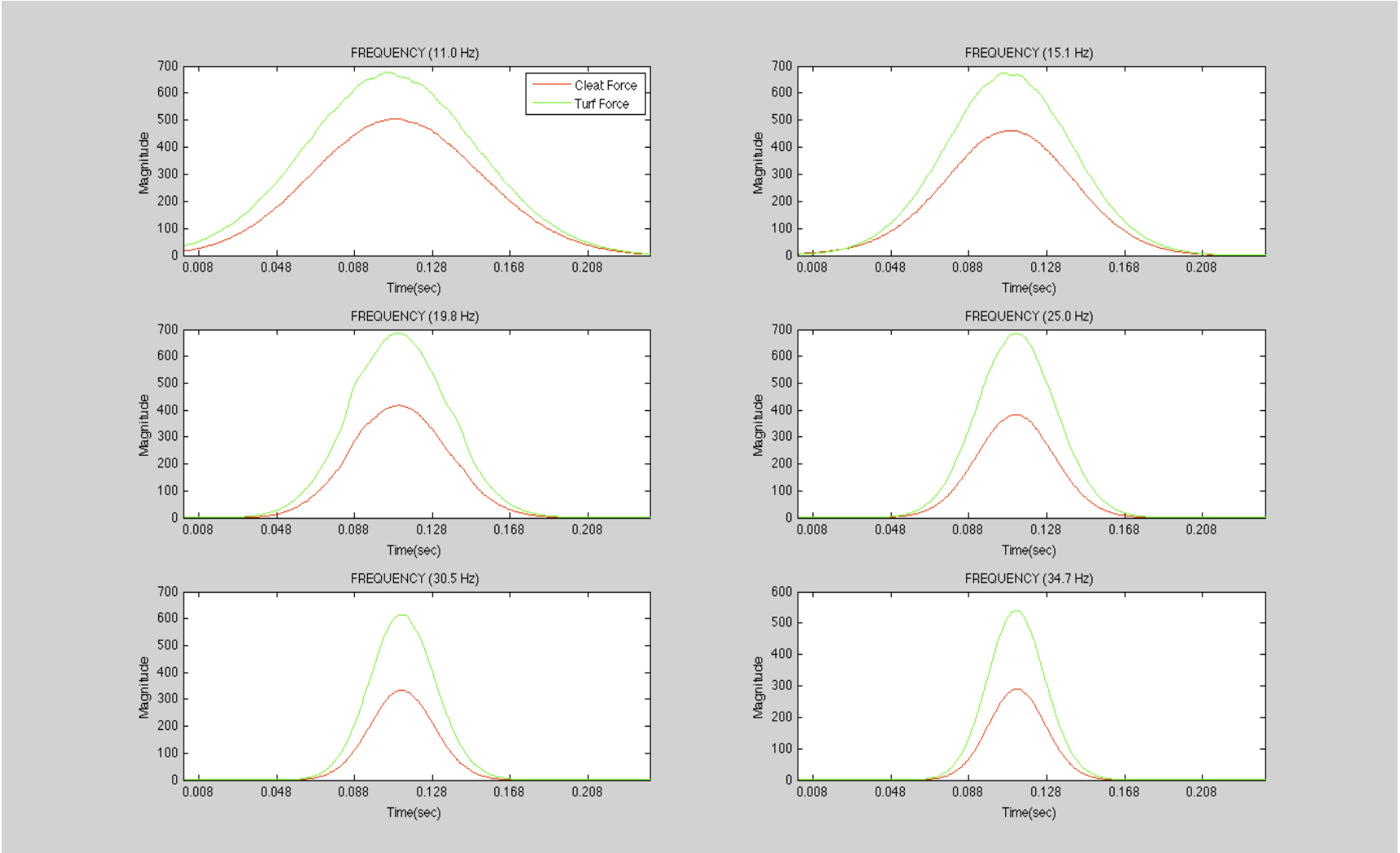

Figure 41. Left Foot Z-Moment Cross-Sections of Power Spectrum from 11 Hz to 35 Hz

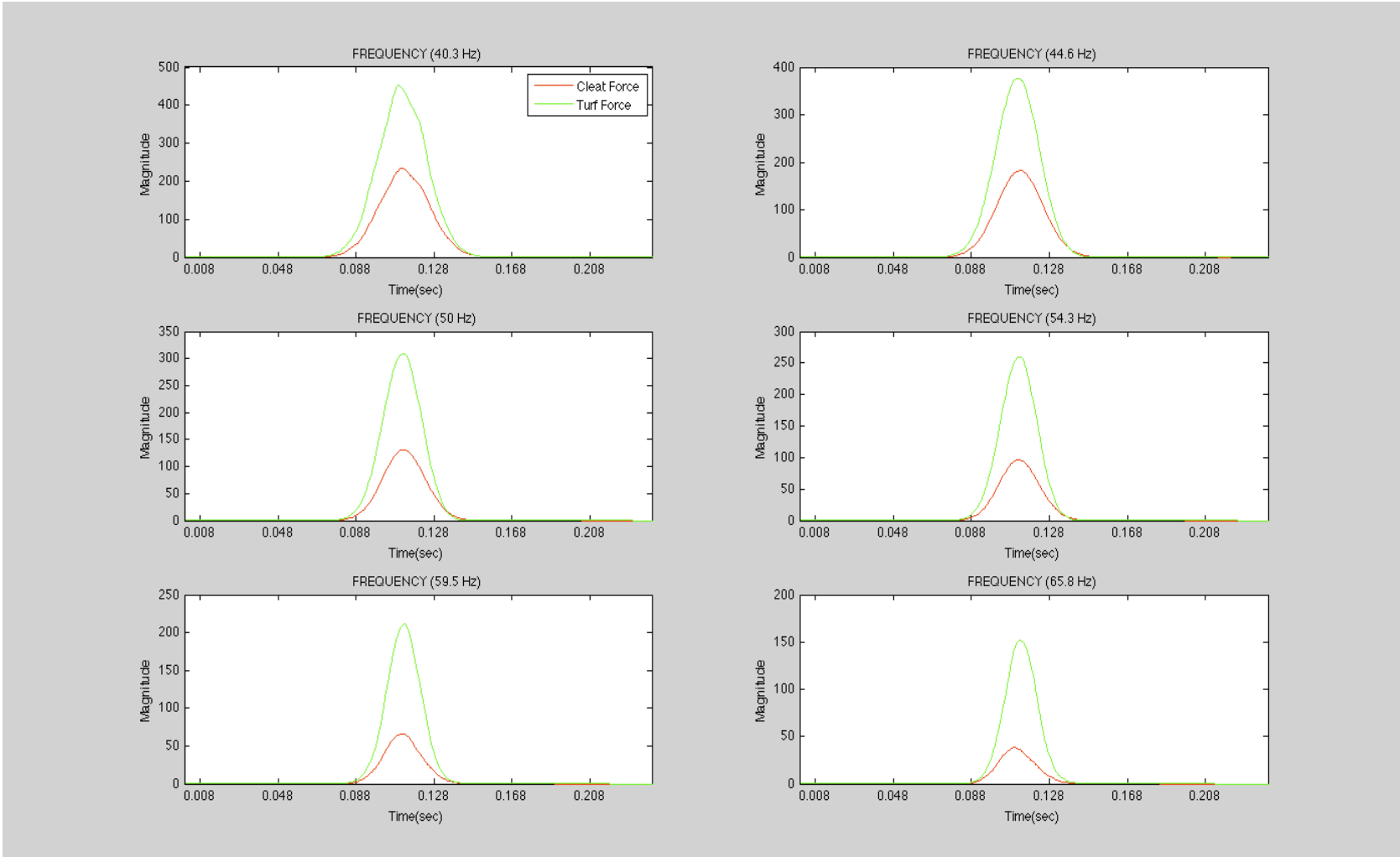

Figure 42. Left Foot Z-Moment Cross-Sections of Power Spectrum from 40 Hz to 65 Hz.

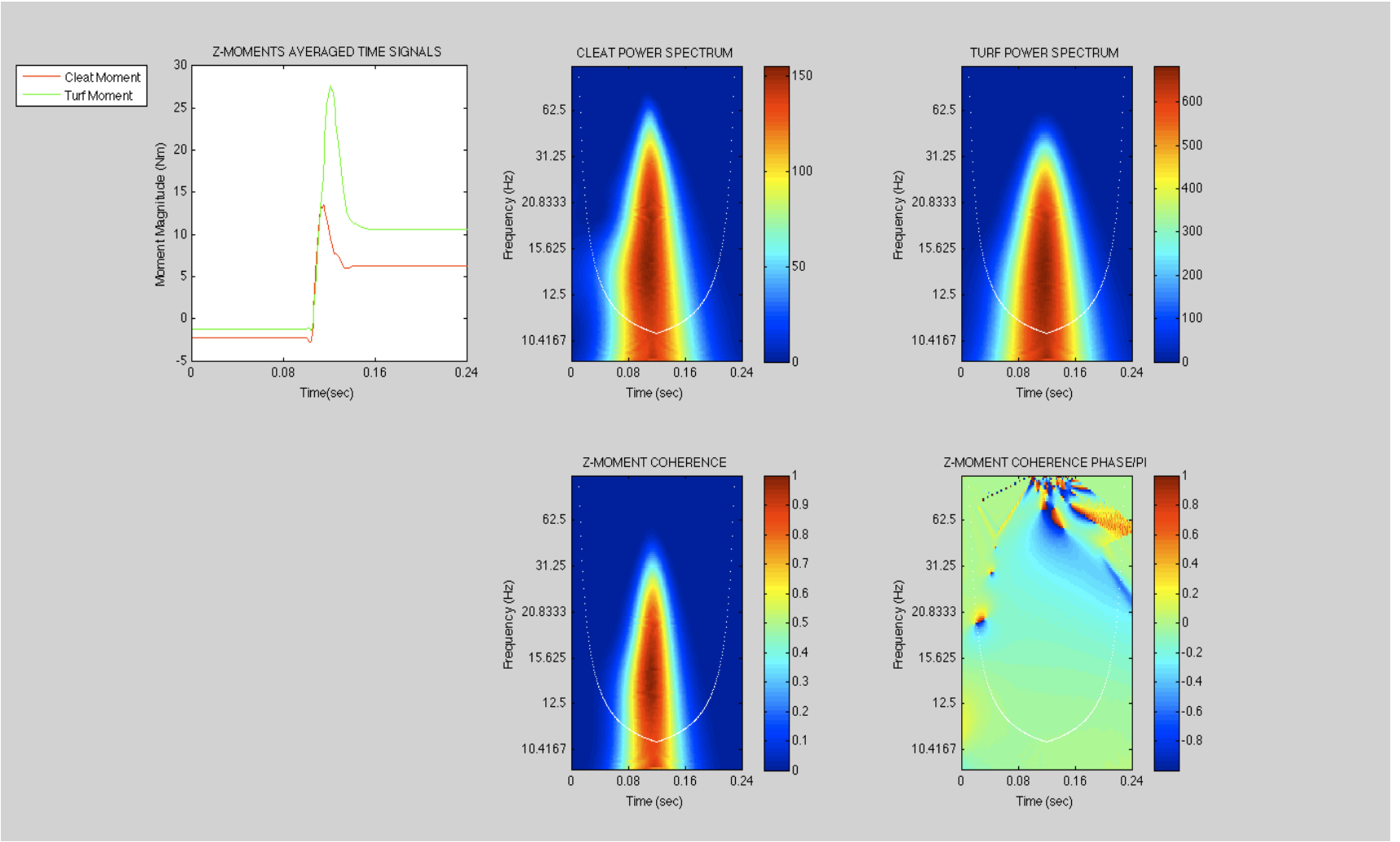

Figure 43. Right Foot Ground Reaction Moment in the Z Direction with CWT Analysis

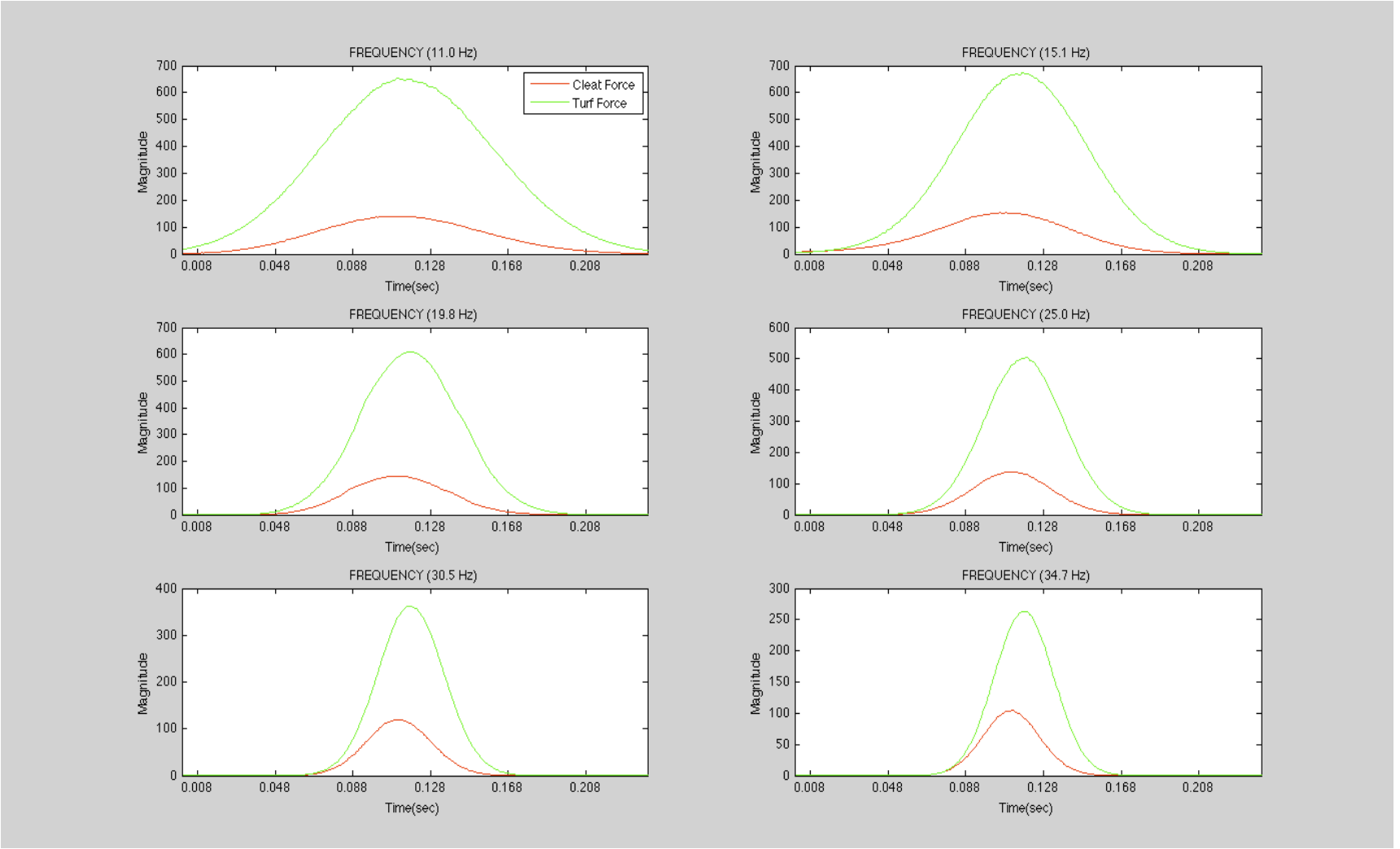

Figure 44. Right Foot Z-Moment Cross-Sections of Power Spectrum from 11 Hz to 35 Hz

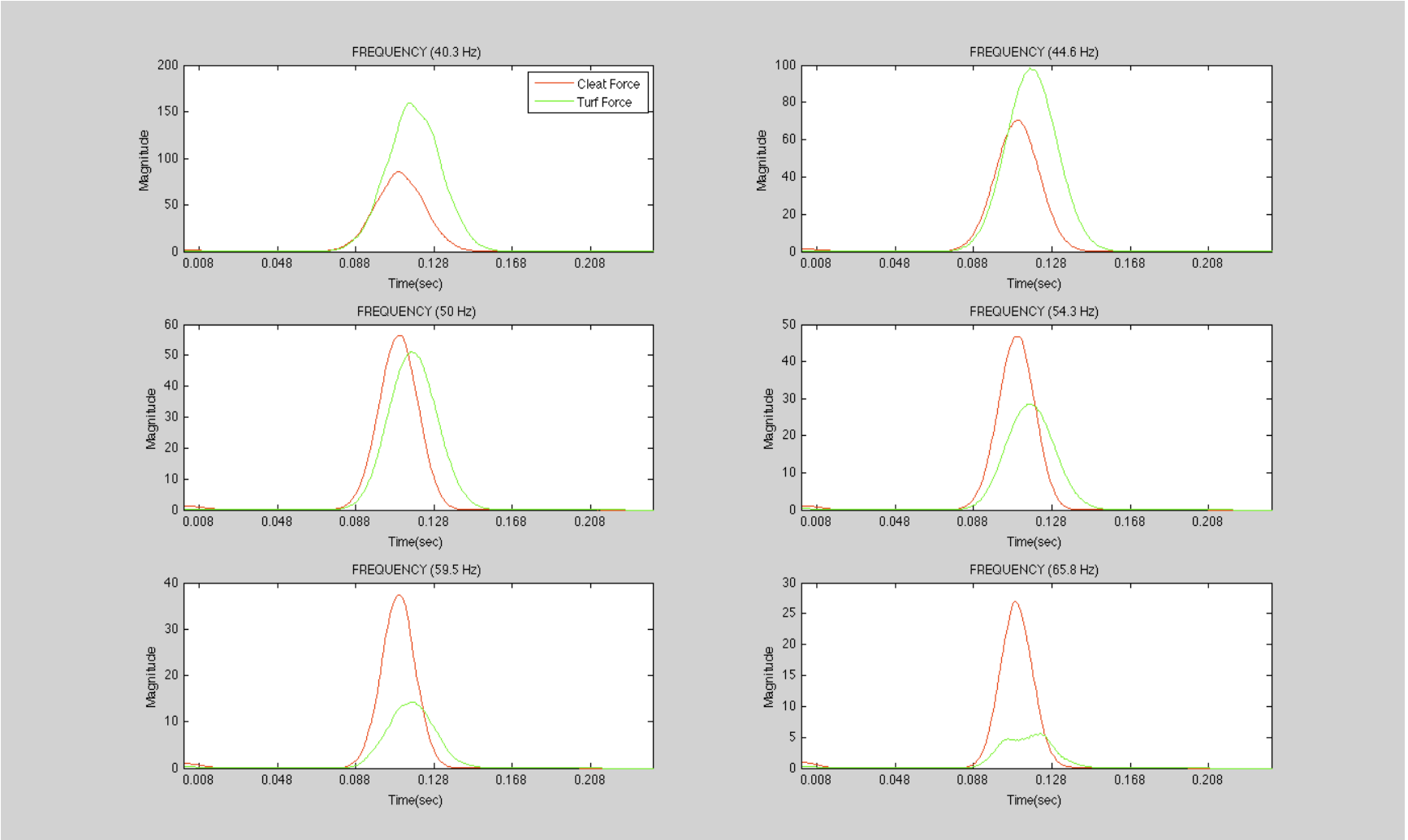

Figure 45. Right Foot Z-Moment Cross-Sections of Power Spectrum from 40 Hz to 65 Hz

As described in the data analysis section of this document, it was possible to summarize and quantitatively characterize the average frequency content of the GRF signals for the left and right foot and the vertical ground reaction moment by plotting the percent differences between maximum values of CWT slices at specified frequencies. From examining the region between the 95% confidence level and the COI of each signal it was verified that the frequency content within the window of 11 to 60 Hz provide valid analytical results.

To read these plots, it is necessary to know that the magnitude of the percent difference is positive when the non-cleated turf shoe has a higher percent difference at a particular frequency. When the magnitude of the percent difference is negative, then the cleated shoe has a higher percent difference, which only occurs in the anterior-posterior (Y-Force) of the right foot and only slightly in the medio-lateral axis (X-Force) of the left foot.

As shown in Figure 46 on the next page, the peak percent difference for the vertical GRF (Z-Force) occurs for both the right foot at 15 Hz and 11 Hz for the left foot.

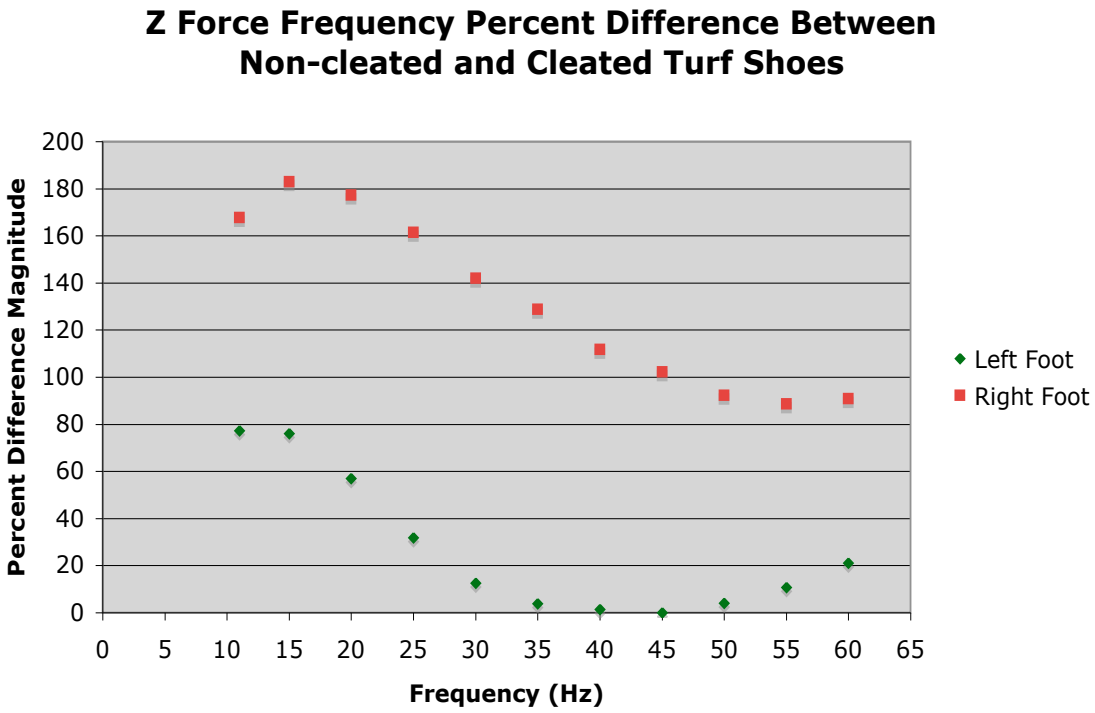

Figure 46. Z Force Frequency Percent Difference Between Non-Cleated and Cleated Turf Shoes

For the right foot, the percent difference for the vertical force never goes below 80 percent. Similarly, the pattern occurs for the left foot, but carries with it an overall lower percent difference, and only reaches a close to zero percent difference between 40 and 45 Hz and then increases from there. This percent difference plot shows that the non-cleated turf shoe allows lower frequency content for the vertical GRF (Z-Force) to dominate both feet, and the right foot in particular has a high percent difference.

In contrast, the anterior-posterior (Y-Force) percent differences are much lower overall compared to all other GRF signals. The percent difference is much lower for the left non-cleated turf shoe foot; plus, as shown in Figure 47, the cleated turf shoe dominates the frequency range, with a peak at 15 Hz and approaches a minimum percent difference at 30-35 Hz, and grows in dominance from 35 Hz.

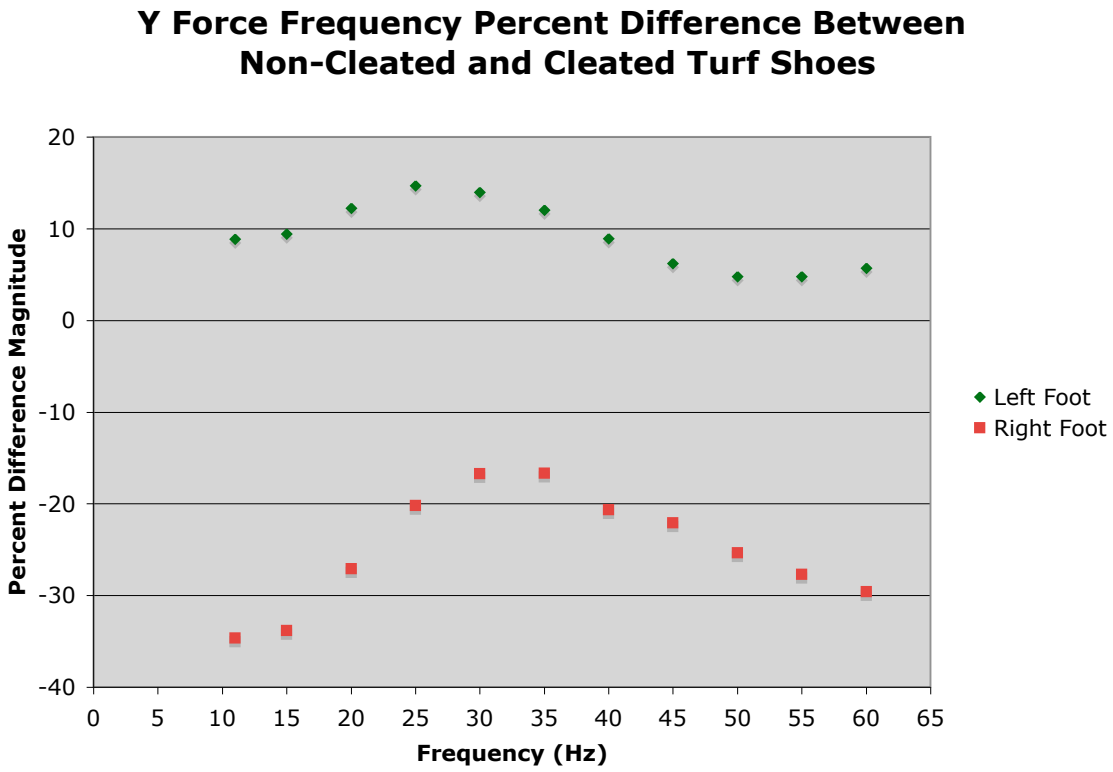

Figure 47. Y Force Frequency Percent Difference Between Non-Cleated and Cleated Turf Shoes

Even though the GRF signal in the medio-lateral (X-Force) direction is on average one-half the normalized body weight of the subjects, there is a very large percent difference of magnitude between the right non-cleated turf shoe and the cleated turf shoe as shown in Figure 48 below. The percent difference plot peaks at 25 Hz, but never goes below the value of 300. For the left foot, the non-cleated turf shoe overwhelmingly dominates from 11 Hz to 25 Hz, whereas the cleated shoe then dominates at a comparatively low percent difference level.

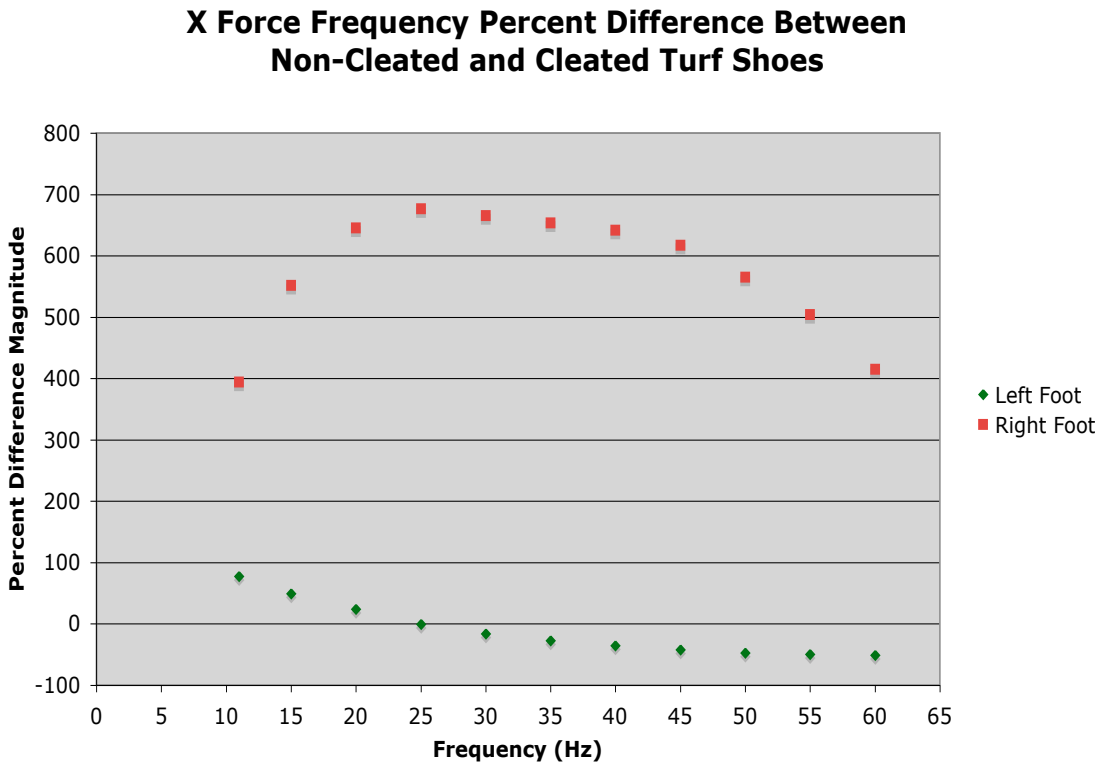

Figure 48. X Force Frequency Percent Difference Between Non-Cleated and Cleated Turf Shoes

The vertical ground reaction moment (Z-Moment) percent difference results, shown on the next page, reveal that again, the non-cleated turf shoe has a much higher magnitude throughout the specified range of frequencies.

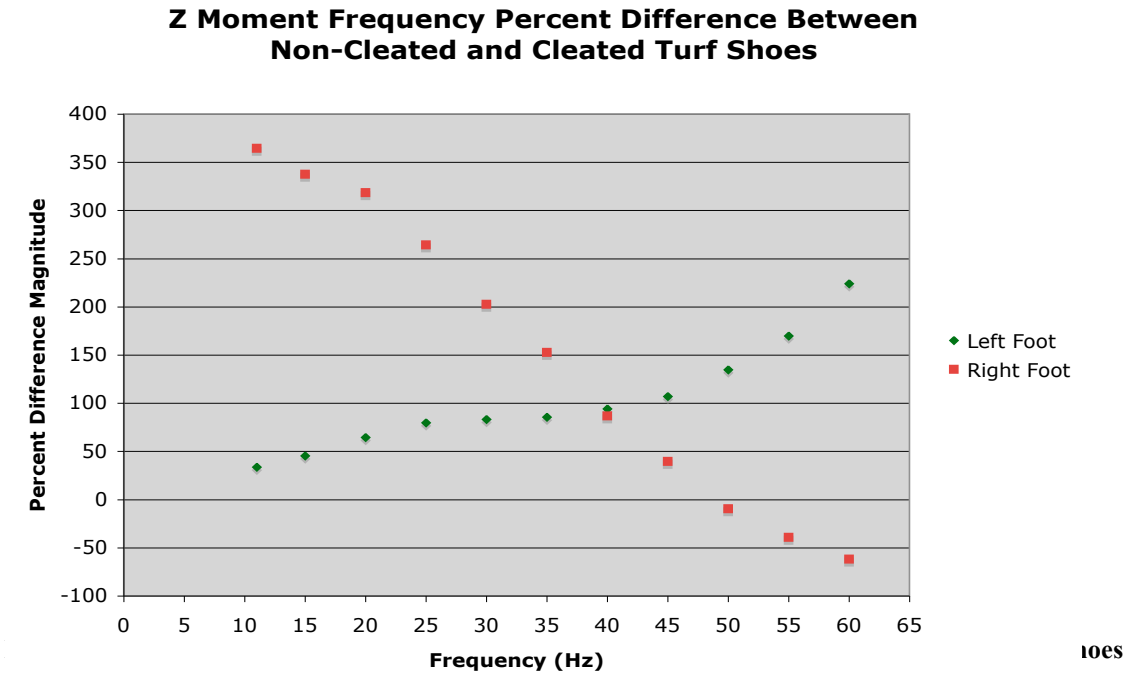

For the right foot, the non-cleated turf shoe has a large percent difference starting at low frequencies and the slope of the percent difference plot decreases until it reaches 50 Hz, where the cleated shoe then has a higher percent difference. For the left foot the non-cleated turf shoe always has a higher percent difference and increases from 33.7 percent difference up to a maximum of 298 percent difference, as shown in Figure 49 below. Consequently, the torque frequency content of both the left and right foot of the non-cleated turf shoe, reflecting the rotational traction of the shoes, is much higher than the cleated shoe between 11 Hz and 50 Hz.

DISCUSSION

The major result of this study is that cross sections of the power spectrum of a CWT can be utilized to characterize and discern frequency content differences between impact GRF signals and vertical moment signals among subjects wearing non-cleated and cleated turf shoes during straight ahead (center) cut and run trials. This result supports the hypothesis of the study that athletes experience different impact force and vertical moment frequency content signals based on the type of shoe they are wearing.

In general, but not always, results show that the magnitudes of impact forces are directly related to the magnitudes of low frequency content between 11 Hz and 60 Hz, and the maximum values of the frequency percent differences vary within each GRF component and the vertical moment plots.

For instance, looking at the magnitudes of the Z force impact signals, the non-cleated turf shoe has an impact level of around 3.5 and 3.0 times percent body weight for the right and left foot respectively, while the cleated shoe has an impact level of around 2.25 and 2.6 percent body weight for the right and left foot respectively. The result of the Z force frequency percent difference plot shows how the non-cleated turf shoe contains a higher level of frequency content for both feet (the right foot in particular) and what is interesting is that for both feet, the maximum value of the percent differences are around 11 to 15 Hz, and this percent difference drops and is a minimum at 55 Hz for the right foot, and 40 Hz for the left foot. For the right foot, where the impact magnitude value is

about one times higher for the non-cleated turf shoe, the percent difference magnitude in frequency content from 11 Hz to 45 Hz is on average over 100% for the same shoe.

This result might lead one to suspect that the magnitude of the impact load always directly relates to the magnitude of the frequency content of the same signal, but looking at the Y force magnitudes and their frequency contents for the right foot in this study, this is not the case. For the Y force, the impact level for the root foot is around 1.65 times percent body weight for both types of shoes, but the Y force percent difference plot shows that the cleated shoe dominates in frequency content in this case with a maximum peak of 35 percent difference around 11 to 15 Hz and has a minimum percent difference of 17 at 30 to 35 Hz. For the left foot, the Y component force for the non-cleated shoe has a slightly higher level, and this is reflected in the Y Force percent difference plot since the percent difference magnitude is slightly higher, but varies with a peak of 14 at 25 Hz, throughout the frequency range of 11 to 60 Hz.

When looking at the X Force, again looking at a situation when the impact loads for the left foot are virtually equal at 0.44 times percent body weight, the intriguing result in the X force percent difference plot is that the non-cleated turf shoe has a higher percent difference between 11 and 20 Hz. Yet, between 25 Hz and 60 Hz, the cleated shoe then has a higher percent difference and the percent difference never goes above 100%.

However, for the right foot, which has an impact load of around 0.47 times percent body weight for the non-cleated shoe and around 0.2 times percent body weight for the cleated shoe weight, the frequency percent difference plot reveals a large difference between the two types of shoes. The magnitude of the percent difference is always above 300% between the frequency ranges of 11 to 60 Hz, and has a peak of 677 percent

difference at 25 Hz. This result stands out from the others and needs further exploration since the impact loads are much lower than the vertical impact loads, and the degree of difference between the maximum values of these loads for the X component compared to the Z component is not much higher, yet produces a much higher percent difference magnitude in the frequency domain.

For the vertical ground reaction moment, the magnitude of the moment seems to again directly relate to the magnitude of the frequency percent difference between the two types of shoes. The non-cleated turf shoe has a higher magnitude for both the right and left feet. The non-cleated turf shoe has a peak moment around 27 Nm and the cleated shoe has a peak moment around 13 Nm for the right foot, thus almost double the torque load. The Z moment frequency percent difference plot shows a large magnitude percent difference for the non-cleated turf shoe, peaking at 365 percent difference at 11 Hz and drops to 0 percent difference between the range of 15 Hz to 40 Hz, where the cleated shoe surprisingly then has a higher percent difference between 50 and 60 Hz. For the left foot, the general pattern holds true showing that for the non-cleated turf shoe, which has a higher moment of -38 Nm contrasted to – 28 Nm for the cleated shoe, the Z moment percent magnitude plot shows that the non-cleated turf shoe always dominates the frequency content. In contrast to all the other GRF components, the percent difference plots for the Z moment of the left foot has a minimum at 11 Hz and increases steadily and has a maximum value of 224 percent difference at 60 Hz.

These results are important because they reveal that the magnitude of the impact forces in general increase the frequency content being transferred to the foot and the lower limbs of the body. Consequently, although the two types of signals in this study on

average were not significantly different, the non-cleated turf shoe showed a higher percentage of frequency content entering the foot in the Z and X component directions, and through the vertical moment.

These results are counterintuitive since the non-cleated turf shoe has a softer heal, which would normally imply that the harder heel of the cleated shoe would transmit more frequency, or at least more of the higher frequencies. Plus, the vertical moment result directly contradicts Villwock's recent work showing that the "turf cleat produced significantly lower torque than [four] other groups" of patterned football shoes [44].

Blurring out distinct features of the subjects when taking the average of the trials and then averaging them together could have possibly created both of these counterintuitive results. For instance, by looking more closely at each particular group of trials, and statistically analyzing them and throwing out outliers from the overall group might reveal a clear picture of events. Overall though, the averaging process gives us a general idea of what is occurring, and these results for this study show that non-cleated turf shoes attenuate the impact forces less and allow a great percent of frequency content to enter the lower limbs of the body.

Another important explanation for these results is that the exact height from which the subject jumped and impact the force plates could have varied. If the subjects on average jumped higher over the level bar during the trial runs when they were wearing the non-cleated turf shoes, then the impact forces for those cases would have been higher. In this study the maximum height was not determined for each individual.

Another important factor that could influence the results is that the landing pattern of the subjects could also have differed depending on the type of shoe they were wearing, or

even the particular psychological moment for the athlete. Both, the actual height from which the athlete dropped and their landing patterns major are factors that could lead to errors when attempting to interpret the results.

Consequently, there are several limitations to this study that future researchers may improve upon. First of all, it would be important to examine the shoes in isolation from the athlete wearing them. That way, controlled heights and impact loads could be created to discern the magnitudes of the percent differences between the two shoes. If the setup were to involve athletes, then it would also be important to somehow have a standard height to drop from onto the force plates, and also capture data on how the subjects are landing onto the force plates. By doing this, then it would be possible to correlate landing patterns to frequency content for each type of shoe. Future studies should also collect data on whether or not the subjects primarily use their right foot to push off with when running, or their left foot since this might influence how the subjects lands in the first place.

Secondly, only the impact portion of the signal was taken into consideration. This was decided upon because the primary frequency content was contained in the impact portion and made it possible to take sections of the CWT and find the percent difference between the peaks, but it is possible that other pertinent frequency content information exists throughout the signal during push off. So, exploring how to analyze and quantify the entire GRF and vertical moment signals (from heel on to toe off) rather than just using the point of impact as a means of discerning differences, would be an important development.

And last of all, one significant limitation of this study was that data was gathered

from only 8 male subjects; and, we see in the study done by Hootman, that the injury rate to the lower extremities is a maximum of 35.9 per 1000 athletes [4]. Hootman's study had a confidence interval of 95% when considering "slightly more than 1 million exposure records", which would indicate that a future study should have a similar sample size. So, a larger sample size is required with the purpose of building a base reference signal for cleated and non-cleated turf shoes.

Overall, one of the more intriguing aspects about this study that is unclear and should be addressed in later studies is how the frequency content entering the lower limbs can be greater for certain shoe even if the impact levels are the same on average. In this study the magnitude of impact signals for the right foot in the Y force direction, and the left foot in the X force direction were the same, yet the frequency content entering the body was different. The reasons for this difference must involve the characteristics of the shoe itself, along with other parameters such as landing pattern, and deserves further study.

In addition to this main interesting aspect, there are two follow up questions that could be explored in future studies. The first would be easy to answer and the second would be more difficult. The first is, "what do the left and right cut and run trials look like when analyzed with this technique?" Since this data was part of the original data set gathered, it would be just a matter of performing the same data preparation and data analysis techniques to these other sets, and comparing and contrasting the results. Of course, the same limitations would apply, but the results would be worth examining.

The second more important and interesting follow up question is, "Is it possible that the peaks of the lower frequencies are near the resonant frequencies of the soft tissues of the lower extremities or near the frequencies when the mechanical impedance of the body

as a whole is a minimum?" Since the soft tissue natural frequency components of the foot are not specifically known at present time, they deserve further study to elucidate the consequences of different low frequency content for cleated and non-cleated athletes. This line of reasoning is substantiated by the study done by Boyer and Nigg, showing how the frequencies of minimum impedance and maximum transmissibility of lower extremity muscle groups were found to be in the range of 5 to 50 Hz [25].

Transmissibility describes the factor of the force input magnitude which is transferred to the mass being observed and it is theorized that muscle damage can occur at these frequencies of maximum transmissibility, which generally coincide with the natural frequency of the system, as the magnitude of the landing is amplified in the muscles [25]. Plus, it is important to recall (shown previously in Figure 7) that Boyer and Nigg found peaks of the mean transmissibility for the Quadriceps (11 Hz and 35 Hz), the Hamstrings (11-15 Hz, and 35 Hz) and the Triceps Surae muscle group (11 Hz and 35 Hz), which all reside in the same low frequency range described by the percent difference plots in this study. Since the frequencies of the transient impact forces, ranging from 11 to 60 Hz, are near the resonant frequency when the mechanical impedance of the lower limb is a minimum then exploring this question in a future study is justified.

CONCLUSION

This study shows that cross sections of the power spectrum of a CWT can be utilized to characterize and discern frequency differences between impact GRF signals and vertical moment signals among subjects wearing cleated and non-cleated turf shoes during straight ahead (center) cut and run trials.

For this study, results show that the percent difference for the vertical GRF is dominated by the non-cleated turf shoes around 11 Hz for both the left and right foot. For the anterior-posterior direction (Y-Force) the non-cleated turf shoe for the left foot has a percent difference peak near 25 Hz, and in contrast for the right foot, the cleated turf shoe has a percent difference peak near 11 Hz. The medial-lateral (X-Force) percent difference plots have large percent difference peaks dominated by the non-cleated turf shoe around 11 Hz for the left foot and 25 Hz for the right foot. The vertical ground reaction torque (Z-Moment) percent difference plot is again largely dominated by the non-cleated turf shoe near 65 Hz for the left foot and 11 Hz for the right foot.

Overall, this study supports the view that athletes experience different impact force and vertical moment frequency content signals based on the type of shoe they are wearing and the main take home message is that in general, but not always, that the magnitudes of impact forces are directly related to the magnitudes of low frequency content between 11 Hz and 60 Hz, and the maximum values of the frequency percent differences vary within each GRF component and the vertical moment plots.

The most intriguing aspect of the study is to examine in future studies why and how

greater amounts of frequency content can enter the lower limbs of the body even when the impact loads for each particular shoe is the same.

REFERENCES

[1] Dickinson, J. A., Cook, S. D., and Leinhardt, T. M., 1985, "The measurement of shock-waves following heel strike while running," Journal of Biomechanics, 18(6), pp. 415-422.

[2] Coermann, R. R., 1962, "The mechanical impedance of the human body in sitting and standing position at low frequencies," Human Factors, 4, pp. 227-253.

[3] Orendurff, M. S., Rohr, E. S., Segal, A. D., Medley, J. W., Green, J. R., and Kadel, N. J., 2008, "Regional foot pressure during running, cutting, jumping, and landing," American Journal of Sports Medicine, 36(3), pp. 566-571.

[4] Hootman J.M., D. R., Agel J., 2007, "Epidemiology of Collegiate Injuries for 15 Sports: Summary and Recommendations for Injury Prevention Initiatives.," Journal of Athletic Training, 42(2), pp. 311-319.

[5] Ohlson, B. a. P. L. O. C., 2007, "Turf Toe," emedicine.medscape.com.

[6] Mullen, J. E., and O'Malley, M. J., 2004, "Sprains - residual instability of subtalar, lisfranc joints, and turf toe," Clinics in Sports Medicine, 23(1), pp. 97-121.

[7] O'Leary, K., Vorpahl, K. A., and Heiderscheit, B., 2008, "Effect of cushioned insoles on impact forces during running," Journal of the American Podiatric Medical Association, 98(1), pp. 36-41.

[8] Shorten, M. R., 2002, "The myth of running shoe cushioning," Proceedings of 4th International Conference on The Engineering of Sport, BioMechanica LLC, Kyoto.

[9] Sammarco, G. J., 1989, "Biomechanics of the foot," Basic biomechanics of the musculoskeletal system, M. Nordin, and V. Frankel, eds., Lea & Febiger, Philadelphia, pp. 163-181.

[10] Gross, T. S., and Nelson, R. C., 1988, "The shock attenuation role of the ankle during landing from a vertical jump," Medicine and Science in Sports and Exercise, 20(5), pp. 506-514.

[11] Whittle, M. W., 1999, "Generation and attenuation of transient impulsive forces beneath the foot: a review," Gait & Posture, 10(3), pp. 264-275.

[12] Title, C. I., and Katchis, S. D., 2002, "Traumatic foot and ankle injuries in the athlete," Orthopedic Clinics of North America, 33(3), pp. 587-589.

[13] Nigg, B. M., 2001, "The role of impact forces and foot pronation: A new paradigm," Clinical Journal of Sport Medicine, 11(1), pp. 2-9.

[14] Wakeling, J. M., Nigg, B. M., and Rozitis, A. I., 2002, "Muscle activity damps the soft tissue resonance that occurs in response to pulsed and continuous vibrations," Journal of Applied Physiology, 93(3), pp. 1093-1103.

[15] Jarrett, M. O., Moore, P. R., and Swanson, A. J. G., 1980, "Assessment of gait using components of the ground reaction force vector," Medical & Biological Engineering & Computing, 18, pp. 685-688.

[16] Simon, R., Paul, I. L., Mansour, J., Munro, M., Abernethy, P. J., and Radin, E. L., 1981, "Peak dynamic force in human gait," Journal Biomechanics, 14(12), pp. 817-822.

[17] Munro, C. F., Miller, D. I., and Fuglevand, A. J., 1987, "Ground reaction forces in running - A reexamination," Journal of Biomechanics, 20(2), pp. 147-155.

[18] Begg, R. K., Sparrow, W. A., and Lythgo, N. D., 1998, "Time-domain analysis of foot-ground reaction forces in negotiating obstacles," Gait Posture, 7(2), pp. 99-109.

[19] Acharya, K. R. H., G.F. Riedel, S.A., and Kazarian, L., 1989, "Force magnitude and spectral frequency content of heel strike during gait," Engineering in Medicine and Biology Society, 1989. Images of the Twenty-First Century., 1989, Seattle, WA, pp. 826-827.

[20] Giakas, G., and Baltzopoulos, V., 1997, "Time and frequency domain analysis of ground reaction forces during walking: An investigation of variability and symmetry," Gait & Posture, 5(3), pp. 189-197.

[21] Stergiou, N., Giakas, G., Byrne, J. E., and Pomeroy, V., 2002, "Frequency domain characteristics of ground reaction forces during walking of young and elderly females," Clinical Biomechanics, 17(8), pp. 615-617.

[22] Wakeling, J. M., Von Tscharner, V., Nigg, B. M., and Stergiou, P., 2001, "Muscle activity in the leg is tuned in response to ground reaction forces," Journal of Applied Physiology, 91(3), pp. 1307-1317.

[23] Boyer, K. A., and Nigg, B. M., 2006, "Muscle tuning during running: Implications of an un-tuned landing," Journal of Biomechanical Engineering-Transactions of the Asme, 128(6), pp. 815-822.

[24] Wakeling, J. M., Liphardt, A. M., and Nigg, B. M., 2003, "Muscle activity reduces soft-tissue resonance at heel-strike during walking," Journal of Biomechanics, 36(12), pp. 1761-1769.

[25] Boyer, K. A., Nigg, B. K., 2007, "Changes in muscle activity in response to different impact forces affect soft tissue compartment mechanical properties.," Journal of Biomechanical Engineering-Transactions of the Asme, 129(4), pp. 594-602.

[26] Hight, T. K., Piziali, R. L., and Nagel, D. A., 1978, "Natural frequency analysis of a human tibia," Journal Biomechanics, 13, pp. 139-147.

[27] Hobatho, M. C., Lowet, G., Cornelissen, M., Cunningham, J., Van Der Perre, G., and Morucci, J. P., 1992, "Determination of resonant frequencies and mode shapes of human tibiae in vivo," Proceedings of the Annual International Conference of the IEEE, pp. 18-19.

[28] Wang, T. G., Hsiao, T. Y., Wang, C. L., and Shau, Y. W., 2007, "Resonance frequency in patellar tendon," Scandinavian Journal of Medicine & Science in Sports, 17(5), pp. 535-538.

[29] Nokes, L. D. M., Williams, J. H., Fairclough, J. A., Mintowtczyz, W. J., and Mackie, I. G., 1984, "A literature review of vibrational analysis of human limbs," Ieee Transactions on Biomedical Engineering, 31(2), pp. 187-192.

[30] Griffin, M. J., 1990, "Whole-body Biodynamics," Hankbook of Human Vibration, Academic Press Limited, San Diego.

[31] Holmlund, P., and Lundstrom, R., 2001, "Mechanical impedance of the sitting human body in single-axis compared to multi-axis whole-body vibration exposure," Clin Biomech (Bristol, Avon), 16 Suppl 1, pp. S101-110.

[32] Misiti, M., 2005, "Wavelet Toolbox User's Guide," The MathWorks, Inc.

[33] Addison, P. S., 2002, The illustrated wavelet transform handbook, Institute of Physics Publishing, Bristol.

[34] Torrence, C., and Compo, G. P., 1998, "A practical guide to wavelet analysis," Bull. AM Meterological Soc., 79(1), pp. 61-78.

[35] R2007a, "MATLAB," The MathWorks.

[36] Sloboda, W., and Zatsiorsky, V. M., 1996, "Wavelet Representation of the Ground Reaction Force Data," Proceedings of the ASME Dynamics Systems and Control Division, 58, pp. 917-926.

[37] Verdini, F., Leo, T., Fioretti, S., Benedetti, M. G., Catani, F., and Giannini, S., 2000, "Analysis of ground reaction forces by means of wavelet transform," Clin Biomech (Bristol, Avon), 15(8), pp. 607-610.

[38] Verdini, F., Marcucci, A., Benedetti, M. G., and Leo, T., 2006, "Identification and characterisation of heel strike transient," Gait & Posture, 24(1), pp. 77-84.

[39] 2008, "BioWare," Kistler Group, Winterthur, Switzerland.

[40] Ge, Z., 2007, "Significance tests for the wavelet power and the wavelet power spectrum," Annales Geophysicae, 25(11), pp. 2259-2269.

[41] Cooper, G. R. J., and Cowan, D. R., 2008, "Comparing time series using wavelet-based semblance analysis," Computers & Geosciences, 34(2), pp. 95-102.

[42] Orme, W., 2009, "Personal Interview."

[43] Garcilazo, R., 2007, "Lower Extremity Mechanics During Cutting Tasks in Different Shoe-Turf Combinations," McNair Scholars Research Journal, 3(1), pp. 35-44.

[44] Villwock, M. R., Meyer, E. G., Powell, J. W., Fouty, A. J., and Haut, R. C., 2009, "Football playing surface and shoe design affect rotational traction," Am J Sports Med, 37(3), pp. 518-525.

APPENDIX

MATLAB Software Programs

MATLAB Software Programs

```
************************************************************
% Code written by Wayne Fischer, Wes Orme, and Joe Guarino
% This routine computes a complex Morlet wavelet transform with central frequency and
bandwidth both at 1 Hz
************************************************************
% *** Inputs;
% *** t             Sample Space (time)
% *** y1,y2         Datasets to be compared
% *** nscales       No. of scales to use
************************************************************
      dt=0.0008;
      t1=500;
      t=1:t1;
      fileaxis=input('Input the axis being evaluated (i.e. X,Y,Z):  ','s');
     %Input the base name of the file
      nscales=128;
      order=9;
      a=0;lsnum=49;
      stepvectors=-1:(2/14):1;
      N=300;
      NL=15

%Perform the wavelet transforms and compute the semblance
      c1=cwt(y1,1:nscales,'cmor1-1');   % Compute the Complex Continuous Transform
      c2=cwt(y2,1:nscales,'cmor1-1');   % Compute the Complex Continuous Transform
      ctc=c1.*conj(c2); ct=abs(ctc);      % Cross wavelet transform amplitude
      spt=atan2(imag(ctc),real(ctc));     % Cross wavelet phase
      order=abs(order); order=floor(order/2)+1; % Check the user input a valid order
      s=cos(spt); s=s.^order;                    % Semblance
      cp=spt/pi;                                 % Coherence Phase divided by Pi
      d=s.*ct;                                   % Dot product

%Plot the two cleat and turf signals
     subplot(3,3,1); plot(y1, 'r'); xlim([0 300]);hold all;   plot(y2, 'b'); xlim([0 300]); hold
     off;
     titlename1=strcat(fileaxis,'-FORCES AVERAGED TIME SIGNALS');
     title(titlename1);
     axis square
     ax=get(gca,'XTicklabel');
     Bnum=str2num(ax);
     BF=dt*Bnum;
     set(gca,'XTicklabel',BF);
     legend('Cleat Force','Turf  Force','Location','NorthWestOutside')
     xlabel('Time(sec)')  ylabel('Normed Magnitude')
```

```
%Plot of Power Spectrum of the Cleat Signal
      subplot(3,3,2);
      imagesc(abs(c1).^2), colormap(jet); xlim([0 300]);
      title('CLEAT POWER SPECTRUM')
      ay=get(gca,'YTicklabel');
      Anum=str2num(ay);
      AF=scal2frq(Anum,'cmor1-1',dt);
      set(gca,'YTicklabel',AF);
      set(gca,'XTicklabel',BF);
      colorbar('location','eastoutside')
      xlabel('Time (sec)')
      ylabel('Frequency (Hz)')
      hold on

%Calculate and plot cone of influence for Cleat Shoe
      for coi_t = 1:NL
      plot(coi_t,128-1.373/(coi_t*dt),'white');%plot left side of coi
      end
      N2L=NL+1;
      for coi_t = N2L:N
      plot(coi_t,128-1.373/((Ncoi_t)*dt),'white');

%plot right side of coi
      end
      hold off

%Plot of Power Spectrum of the Turf Signal
     subplot(3,3,3);
     imagesc(abs(c2).^2),colormap(jet); xlim([0 300]);
     title('TURF POWER SPECTRUM')
     colorbar('location','eastoutside')
     set(gca,'YTicklabel',AF);
     set(gca,'XTicklabel',BF);
     xlabel('Time (sec)')
     ylabel('Frequency (Hz)')
     hold on

%Calculate and plot cone of influence for Cleat Shoe
       for coi_t = 1:NL  plot(coi_t,128-1.373/(coi_t*dt),'white');
%plot left side of coi
       end
       N2L=NL+1;
       for coi_t = N2L:N
       plot(coi_t,128-1.373/((N-coi_t)*dt),'white');
```

```
%plot right side of coi
        end
        hold off

%Plot Max Power vs Frequency
        subplot(3,3,4);
        c1flip=flipud(c1);
        c2flip=flipud(c2);
        FA=flipud(AF);
        plot(max(abs(c1flip).^2,[],2), 'r'); xlim([1 128]); hold all;
        plot(max(abs(c2flip).^2,[],2), 'b'); xlim([1 128]); hold off;
        set(gca,'XTicklabel',FA);
        title('MAXIMUM POWER VS FREQUENCY')
        xlabel('Frequency (Hz)')
        ylabel('Maximum Power')

%Plot Max Power vs Time
        subplot(3,3,5);
        plot(max(abs(c1).^2), 'r'); xlim([0 300]); hold all;
        plot(max(abs(c2).^2), 'b'); xlim([0 300]); hold off;
        title('MAXIMUM POWER VS TIME');
        axis square
        set(gca,'XTicklabel',BF);
        xlabel('Time (sec)')
        ylabel('Maximum Power')

%titlename=strcat(fileaxis,filefm,fileleg,' X WAVELET POWER');
subplot(3,3,7); contourf(ct); title(titlename); colorbar('location','eastoutside')
        ch=(abs(ctc)).^2;ch=ch/max(max(ch));       %Coherence
        titlename=strcat(fileaxis,'-FORCE',' COHERENCE');
        subplot(3,3,6);
        imagesc(ch); xlim([0 300]);
        title(titlename);
        colorbar('location','eastoutside')
        set(gca,'YTicklabel',AF);
        set(gca,'XTicklabel',BF);
        xlabel('Time (sec)')
        ylabel('Frequency (Hz)')
        hold on

%Calculate and plot cone of influence for Cleat Shoe
        for coi_t = 1:NL
        plot(coi_t,128-1.373/(coi_t*dt),'white');
```

```
%Plot left side of coi
        end
        N2L=NL+1;
        for coi_t = N2L:N
        plot(coi_t,128-1.373/((N-coi_t)*dt),'white');

%Plot right side of coi
        end
        hold off
        titlename=strcat(fileaxis,'-FORCE',' COHERENCE PHASE/PI');
        subplot(3,3,7);
        imagesc(cp);xlim([0 300]);
        title(titlename);
        colorbar('location','eastoutside')
        set(gca,'YTicklabel',AF);
        set(gca,'XTicklabel',BF);
        xlabel('Time (sec)')
        ylabel('Frequency (Hz)')
        hold on

%Calculate and plot cone of influence for Cleat Shoe
        for coi_t = 1:NL
        plot(coi_t,128-1.373/(coi_t*dt),'white');

%Plot left side of coi
        end
        N2L=NL+1;
        for coi_t = N2L:N
        plot(coi_t,128-1.373/((N-coi_t)*dt),'white');

%Plot right side of coi
        end
        hold off
```